

Katja Sallinger BSc

**Molecular and cellular response of curcumin on human soft  
tissue sarcoma cell lines**

**MASTER'S THESIS**

to achieve the university degree of

Master of Science

Master's degree programme: Biochemistry and Molecular Biomedical Sciences

submitted to

**Graz University of Technology**

Supervisor

PD Mag. Dr. Birgit Lohberger

Department of Orthopedics and Trauma,

Medical University of Graz

Graz, August 2017

## AFFIDAVIT

I declare that I have authored this thesis independently, that I have not used other than the declared sources/resources, and that I have explicitly indicated all material which has been quoted either literally or by content from the sources used. The text document uploaded to TUGRAZonline is identical to the present master's thesis.

Date

Signature

## Dedication

I dedicate this work to my lovely family members, who passed away too early and can't share this moment with me.

## Acknowledgement

First of all, I would like to thank my supervisor Dr. Birgit Lohberger, for the opportunity to write this thesis and the support during the whole time. I also want to thank my colleagues Heike Kaltenecker and Nicole Stündl for their help and patience during my time in the laboratory.

My greatest appreciation goes to my parents Sigrid, Josef and the rest of my family, who supported me in every possible way during my whole studies and made my student days to an unforgettable and also carefree experience.

I want to say a special thank to my friends Nina, Tanja and Bixi and my boyfriend Bernhard, who supported me during my whole lifetime and always believed in me.

## Abstract

Synovial sarcoma (SS) is a high-grade, malignant soft tissue sarcoma (STS) accounting for 5–10% of STS. After rhabdomyosarcoma, SS is the most common STS in children, adolescents, and young adults. Osteosarcoma is a deadly form of musculoskeletal cancer that most commonly causes patients to die of pulmonary metastatic disease. The development of new therapeutic agents targeting the malignant behaviour of synovial- and osteosarcoma cells is important to improve the prognosis.

Curcumin a yellow pigment and spice in turmeric and curry, exhibits anticarcinogenic effects. However the anticarcinogenic effect of curcumin on synovial sarcoma and osteosarcoma cells are mostly unknown.

With this study it could be shown that in the sarcoma cell lines SW-982 and U2OS curcumin decreased the cell viability and the cell proliferation in a dose dependent manner. The apoptotic behaviour of both cell lines was examined by FACS analysis and was confirmed by Western Blot analysis of the gene expression of cleaved PARP, which was used as an indicator for apoptosis. No apoptotic effect could be observed in the SW-982 cells and only a very low one in the U2OS cells, concerning 9.5% of all U2OS cells.

In addition a proteome profiler array (NF $\kappa$ B-assay) was performed to determine the relative levels of selected human NF $\kappa$ B proteins. With four of these highly expressed genes (FADD, FAS, DR4 and TNFR1) a quantitative Real-time Polymerase Chain Reaction was performed, which showed an increase of all four genes in curcumin treated SW-982 and U2OS cells. The expression of H2AX, an indicator for cell damage, was examined by Western Blot analysis. In both cell lines the expression was increased in curcumin treated cells, which led to the conclusion that curcumin induces cell damage in both cell lines. Many different types of human tumors have misregulated NF- $\kappa$ B, that NF- $\kappa$ B is constitutively active. The active form of NF $\kappa$ B up-regulates the expression of

genes that keep the cell proliferating and protect the cell from conditions that would cause the cells to die. Treatment of the sarcoma cell lines with curcumin showed a decrease in the gene expression of the phosphorylated I $\kappa$ B- $\alpha$  and thus led to an inhibition of the binding of p65-complexes to their cognate binding sites. In contrast to p65 the binding of p50 to NF $\kappa$ B sites was not inhibited, suggesting that the I $\kappa$ B- $\alpha$  family binds to the p65 subunit of p50-p65 hetero complex.

## Zusammenfassung

Das Synovialsarkom ist eine bösartige, mesenchymale Geschwulst, die etwa 5-10% aller Weichgewebssarkome repräsentiert. Nach den Rhabdomyosarkomen zählt das Synovialsarkom zu den am häufigsten auftretenden Weichgewebssarkomen in Kindern und Jugendlichen. Das Osteosarkom ist eine tödlich verlaufende Form einer Krebserkrankung des Bewegungsapparates, bei der die Patienten dann in weiterer Folge an pulmonalen metastatischen Erkrankungen sterben. Die Entwicklung von neuen therapeutischen Medikamenten zur Behandlung des Synovialsarkoms und des Osteosarkoms ist daher essentiell, um die Prognose für Patienten zu verbessern.

Curcumin, ein gelbes Farbpigment und Gewürz, welches in Tumeric und Curry enthalten ist, zeigte in der Vergangenheit bereits verschiedene antikarzinogene Eigenschaften. Jedoch ist es noch weitgehend unbekannt, wie sich die antikarzinogenen Eigenschaften von Curcumin auf Synovialsarkome und Osteosarkome auswirken.

In dieser Arbeit konnte gezeigt werden, dass die Lebensfähigkeit und das Wachstumsverhalten der Sarkomzelllinien SW-982 und U2OS durch die Behandlung mit Curcumin, in Abhängigkeit der Dosis, abnahm. Das apoptotische Verhalten beider Zelllinien wurde mittels FACS Analyse untersucht und die Ergebnisse wurden durch eine Western Blot Analyse bestätigt, bei der die Genexpression von cleaved PARP gemessen wurde, welches als Apoptosemarker dient. Jedoch konnte in den SW-982 Zellen kein apoptotisches Verhalten und in den U2OS Zellen nur eine geringe apoptotische Aktivität von etwa 9.5% nachgewiesen werden.

Desweiteren wurde ein Proteome Profiler Array durchgeführt, um die Expression bestimmter NFκB-Proteine zu ermitteln. Die Expression vier dieser Proteine (FADD, FAS, DR4 und TNFR1) wurde dann mit qPCR weiteruntersucht, wobei ein deutlicher Anstieg in Curcumin behandelten Zellen zu erkennen war.

Auch die Expression eines Indikators für Zellzerstörung, H2AX, wurde mittels Western Blot Analyse gemessen, wobei wiederum ein Anstieg der Expression in Curcumin behandelten Zellen zu sehen war. Zudem wurde die Auswirkung von Curcumin auf den NF- $\kappa$ B- Stoffwechselweg untersucht, wobei eine verringerte Expression des phosphorylierten I $\kappa$ B- $\alpha$ -Proteins festgestellt wurde, was letztendlich zu einer Bindungsinhibierung des p65-Komplexes an die Bindungsstellen im Zellkern führte. Im Gegenteil zur Inhibierung der Bindung von p65 an seine Kernsequenzen, wurde die Bindung von p50 an seine Sequenzen im Kern nicht inhibiert, was darauf schließen lässt, dass die I $\kappa$ B- $\alpha$  Proteinfamilie an die p65 Untereinheit von p50-p65 Heterokomplexen bindet.

## Table of contents

1	Introduction.....	1
1.1	Types of Cancer .....	1
1.2	The Development of Cancer.....	2
1.3	Sarcomas .....	4
1.3.1	Synovial sarcoma .....	5
1.3.2	Osteosarcoma .....	6
1.4	Curcumin .....	7
1.5	Apoptosis.....	8
1.5.1	Morphology of Apoptosis .....	8
1.5.2	Mechanisms of Apoptosis.....	9
1.5.3	Biochemical Features.....	10
1.5.4	Extrinsic Pathway .....	11
1.5.5	Execution Pathway.....	12
1.6	NF-kappa-B signaling pathway.....	13
2	Methods.....	15
2.1	Cell culture .....	15
2.2	Power Plex® system .....	15
2.3	Vimentin-DAPI Immunofluorescence staining.....	17
2.4	Proliferation assay.....	19
2.4.1	Cell viability assay (MTS assay) .....	19
2.4.2	xCELLigence Real-time cell analysis .....	20
2.5	Measurement of apoptosis by flow cytometry.....	21
2.5.1	Flow cytometer .....	21
2.5.2	Cleaved caspase 3 assay .....	22
2.5.3	Annexin/PI assay.....	23
2.6	Quantitative Real-time Polymerase Chain Reaction.....	24

2.6.1	RNA isolation.....	24
2.6.2	Removal of genomic DNA and cDNA synthesis .....	26
2.6.3	Real-time – quantitative Polymerase Chain Reaction .....	27
2.7	Proteome profiler array (NFκB-assay).....	28
2.8	Western Blot .....	31
2.8.1	Gel casting.....	31
2.8.2	Preparation for the gel casting .....	32
2.8.3	Sample preparation and gel electrophoresis.....	33
2.8.4	Protein transfer:.....	36
3	Results.....	40
3.1	Confirmation of the samples by STR analysis and IHC staining .....	40
3.2	Curcumin reduced cell proliferation and viability of sarcoma cell lines SW-982 and U2OS.....	43
3.3	Curcumin induced apoptosis could not be measured by FACS analysis.....	47
3.4	The proteome profiler array identified the highest expressed NFκB proteins.....	50
3.5	Gene expression of FADD, Fas, DR4 and TNFR1 showed an increase in curcumin treated cells.....	51
3.6	Curcumin induced cell damage but didn't induce apoptosis .....	52
3.7	Curcumin influenced NFκB-pathway.....	53
4	Discussion .....	55
5	References .....	61
6	List of Abbreviations .....	69
7	List of Figures.....	71
8	List of Tables .....	73

# 1 Introduction

## 1.1 Types of Cancer

Cancer can develop from any of the different kinds of cells in the body by abnormal proliferation, so more than a hundred different types of cancer can arise, which differ in their behaviour and response to treatment. The most important distinction in cancer diagnosis is the differentiation between benign and malignant tumors. A tumor is defined as any abnormal proliferation of cells that can be either benign or malignant. A benign tumor stays confined to its original location, does not invade surrounding tissue and does not spread to other body sites. A malignant tumor is showing both of these characteristics, it can invade surrounding normal tissue and can spread through the body via the circulatory or lymphatic system. Only malignant tumors are termed as cancers and their ability to metastasize and invade normal, healthy tissue makes this disease so dangerous. Whereas benign tumors can be treated by surgical removal, the metastasizing feature of malignant tumors to other locations in the body can bedevil the treatment and could grant them resistances to such localized treatments. Both benign and malignant tumors are classified relative to the cell type from which they develop.

Most cancers can be distributed into one of the following main groups: carcinomas, sarcomas and leukemia. Carcinomas are malignancies of epithelial cells, which include about 90% of all human cancers. Sarcomas are solid tumors of connective tissues, such as cartilage, bone and muscle tissue and appear very rarely in humans. Leukemias arise from the blood forming cells and from cells of the immune system and account for approximately 8% of human cancers. Further, tumors can be classified according to the tissue of origin and the type of involved cells. [1]

## 1.2 The Development of Cancer

One of the fundamental characteristics of cancer is the development of tumors from a single cell that begins to proliferate abnormally, which is defined as tumor clonality. In many tumors the single cell origin has been demonstrated by X chromosome inactivation analysis. For example one member of the X chromosome pair is inactivated in female cells by the conversion to heterochromatin. The inactivation of one X chromosome appears during the embryonic development, so one X chromosome is inactivated in some cells while the other one stays active in other cells. Meaning that if a female is heterozygous for an X chromosome gene, different alleles can be expressed in different cells. Normal tissues are built up by a mixture of cells with different inactive X chromosomes, so the expression of both alleles can be measured in normal tissues of heterozygous female beings. In contrast to this fact, tumors normally express only one allele of a heterozygous X chromosome gene. This leads to the conclusion that all the cells building up the tumor are all developing from a single cell of origin, in which the X inactivation pattern was programmed before the tumor began to develop. [1]

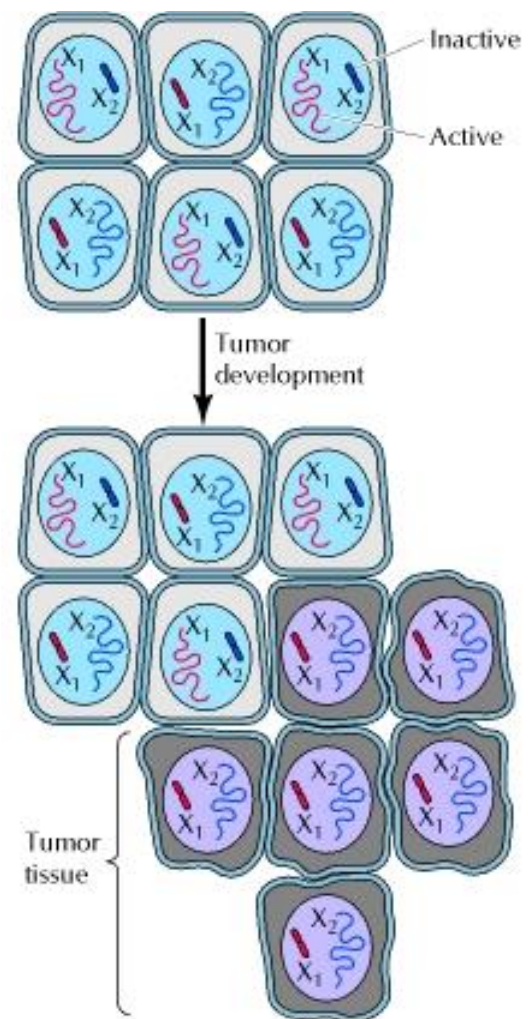
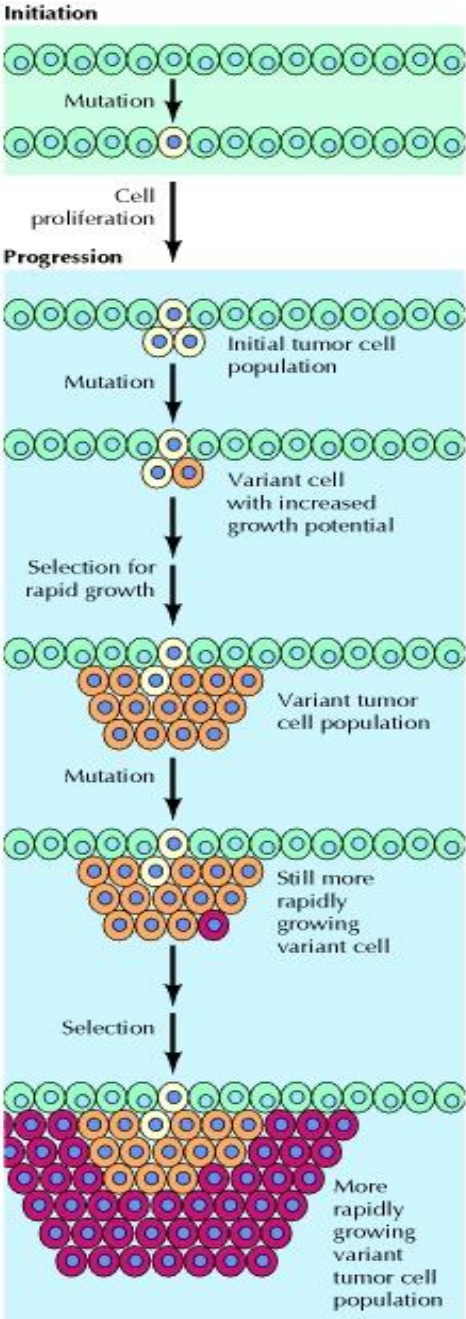


**Figure 1: Tumor clonality**

Normal cell tissue of healthy humans is built up of a mosaic of cells, in which some of the X chromosomes are inactivated and others stay active. A tumor develops from a single cell, so each tumor cell is having the same X chromosome inactivation pattern. (<https://www.ncbi.nlm.nih.gov/books/NBK9963/>, 2017.07.03)

The clonal origin of tumors that develops out of an original progenitor cell does not have to show all of the characteristics of a cancer cell. Rather the development of cancer is known as a multistep process in which the cells develop malignant behaviour through a progressive series of modifications. One characteristic of the multistep development of cancer is that most

cancers develop late in life. To cite one example, the appearance of colon cancer increases more than tenfold between the ages of 30 and 50, and another tenfold between 50 and 70. Such a dramatic increase of cancer incidence with age implies that most cancers develop as a result of multiple abnormalities, which accrue over periods of many years. [1]



The development of cancer can be seen as a multistep process involving selection and mutation for cells with rising capacity for survival, proliferation, invasion and metastasis. Tumor initiation or better known as the first step in the process, is thought to be the consequence of a genetic change leading to abnormal proliferation of a single cell. Cell proliferation then results in the outgrowth of a population of clonally derived tumor cells. Tumor progression proceeds by the appearance of additional mutations within cells of the tumor population. Some of these mutations grant a selective advantage to the cell, such as more rapid growth, and the daughter cells of such a cell showing such a mutation will consequently become dominant within the tumor population. This process is also known as clonal selection in which a new clone of tumor cells has developed on the basis of its increased growth rate or other properties that grant a selective advantage. Clonal selection continues during the process of tumor development, so tumors currently become more and more rapid-growing and show an increasingly malignant behaviour. [1]

**Figure 2: Stages of tumor development**

The development of cancer initiates when a single mutated cell begins to proliferate abnormally. Additional mutations followed by selection for more rapidly growing cells within the population then result in progression of the tumor to increasingly rapid growth and malignancy. ( <https://www.ncbi.nlm.nih.gov/books/NBK9963/>, 2017.07.03)

### 1.3 Sarcomas

Sarcomas belong to a heterogeneous group of very rare tumors, which develop from the embryonic mesoderm. To date, Ewing's sarcomas, bone sarcomas, neuro-ectodermal tumors and soft tissue sarcomas appear most frequently. More than 8000 new cases of soft tissue sarcomas were diagnosed in the United States and more than 3000 deaths from soft tissue sarcomas (STS) were predicted in 2004, accounting for 0.63% of all cancer cases and 1.15% of deaths from cancer. [2]

STS can appear anywhere in the body, but most frequently it develops in the extremities (59%), in the trunk (19%), in the retroperitoneum (15%), or in the head and neck (9%). [3] The most common histological types of STS are malignant fibrous histiocytoma (28%), leiomyosarcoma (12%), liposarcoma (15%), synovial sarcoma (10%) and malignant peripheral nerve sheath tumors (6%), but more than 50 histologic types have been identified. The most common soft tissue sarcoma of childhood are Rhabdomyosarcomas. [4] [Reviewed in 5]

#### Risk factors

One well-established risk factor for developing STS is external radiation therapy by the fact that the incidence of developing sarcomas is increased 8- 50-fold in patients that were treated with radiation therapy for treating another type of cancer such as breast cancer, cervix cancer, ovary cancer or cancer of the lymphatic system. [6, 7] However it could be observed that the risk of developing sarcomas appears proportional with the dose of radiation. Also the exposure to certain chemicals, for example herbicides such as phenoxyacetic acids and wood preservatives containing chlorophenols, could be identified as other risk factors. [8, 9] Also genetic predispositions such as specific inherited genetic alterations are linked with an increased risk of developing bone and STSs. Some of the oncogenes that have been associated in the development of STSs include N-Myc, MDM2, c-erbB2 and some members of the Ras family. In several subtypes of STSs these genes were amplified giving us the result that alterations in these genes correlate with an increased risk. [10] The performance of a cytogenetic analysis of soft tissue tumors has shown particular translocations of chromosomes that code for onco-proteins correlating with certain histologic subtypes. The best examined chromosomal translocations have been observed in the clear-cell sarcoma (EWS–ATF1 fusion), have been seen in the Ewing's sarcoma (EWS–FLI-1 fusion), and have been identified in the alveolar rhabdomyosarcoma (PAX3–FHKR fusion) and in the

synovial sarcoma (SSX–SYT fusion). [11] In the inhibition of cell growth tumor suppressor genes play a critical role, which can suppress the growth of cancer cells. In soft tissue tumors two of these genes are important: the retinoblastoma (Rb) gene and the p53 tumor suppressor gene. If a mutations or deletion in the Rb gene appears, retinoblastomas and sarcomas of the soft tissue and bone can develop. Additionally, mutations in the p53 tumor suppressor gene have also been observed in 30 - 60% of STSs. In patients with germline mutations in the tumor suppressor gene p53 there is also an increased risk of developing STSs. [12, 13] [Reviewed in 5, 14]

### 1.3.1 Synovial sarcoma

Synovial sarcoma (SS) belongs to the group of malignant STSs, which account for 5–10% of STS. [15-17] SS is the second most common STS in children, and young adults, after rhabdomyosarcomas. [16] The definition ‘synovial sarcoma’ descends from the morphological similarity to the embryonic synovialis. [16, 17] In many cases the misinterpretation exists that the tumor origin develops from synovial tissue, which is not the case. [17-19] Myogenic cells have been suggested to be the origin of SS [17] and in the most cases the tumor appears in the lower (62%) and upper (21%) extremities, but actually a development could occur everywhere in the body. [18, 20] SS can be divided into three different histological classes, so the tumors can be biphasic, monophasic or poorly differentiated. [22] In terms of important prognostic factors no distinct facts are known. Although in some studies tumor grade is suggested to be the most important prognostic indicator, in the most studies all SS are classified as high grade tumors and no distinction between grade 2 and grade 3 tumors is done. [23, 24] The existence of the SYT–SSX fusion type is characterized to be a prognostic indicator as well. [24 – 27] But no distinct statement in relation to the predictive role of SYT–SSX fusion type is made yet, in contrast a lot of different conflicting results could be observed. [23, 24] Metastases and a local recurrence can be linked with SS and the occurrence of developing metastases appears in 50–70% of cases. Because of the fact that these grow very slow, a high incidence of the appearance of late metastases exist. Wide resection and chemotherapy in combination with radiation therapy is suggested to be the standard treatment [29-31] but also the removal of the regional lymph nodes is submitted. [32] [Reviewed in 33]

### 1.3.2 Osteosarcoma

Osteosarcoma is known as the most common malignant bone tumor. [34, 35] Primitive mesenchymal bone-forming cells have been suggested to be the origin of OS. The histologic feature that appears to be characteristic for these tumors is the production of malignant osteoid. In addition other cell populations can appear because also these types of cells are able to arise from pluripotential mesenchymal cells. Any occurrence of malignant bone cells is diagnosed as OS. In most cases these tumors, or also defined as musculoskeletal cancer, lead to death and patients die because of developing pulmonary metastatic disease. Fast growing areas of long bones in children are the most common location of development for these tumors, but hypothetical any bone can be affected. The three most affected areas are the distal femur, the proximal tibia and the proximal humerus. [36 - 40] Surgical removal of the malignant area is suggested to be the standard therapy but in most cases limb-sparing techniques can be used to treat patients with OS and maintain the function. For the treatment of micro-metastases that are present in many cases, but not detectable in most patients at the time of diagnosis, chemotherapy is also involved in the standard therapy procedure. [41] Although the exact cause of developing OS is unknown, a number of risk factors exist. [36 – 38] One main predisposition factor for developing OS is rapid bone growth, as it develops frequently during the adolescent growth spurt, and in large-breed dogs. A typical location was identified to be the metaphyseal area adjacent to the growth plate of long bones. [39-43]

Genetic predisposition is also a big risk factor. Bone dysplasias such as enchondromatosis, the Paget disease, retinoblastoma and fibrous dysplasia increase the risk of developing OS. Mutation of the RB gene in combination with radiation therapy is associated with a high risk of developing these type of tumors. Another known risk factor is the existence of the Li-Fraumeni syndrome (germline p53 mutation), and Rothmund-Thomson syndrome (autosomal recessive association of hair and skin dysplasias, bone defects, cataracts and hypogonadism). Exposure to radiation is the only known environmental risk factor. The 5-year survival rate was 63% (59% for males, 70% for females) for patients that were diagnosed between 1974 and 1994. [44 - 48] [Published in 49]

## 1.4 Curcumin

Curcumin is the major active component of turmeric, a yellow compound originally isolated from the plant *Curcuma longa*. As a spice it provides curry with its distinctive colour and flavour. [50]

It was first isolated in 1815, crystallized in 1870, [51, 52] and identified as 1,6-heptadiene-3,5-dione-1,7-bis(4-hydroxy-3-methoxyphenyl)-(1E,6E). While hydroxyl groups in curcumin are required for its antioxidant activity, its methoxy groups are essential for its anti-inflammatory and anti-proliferative activity. Various molecular targets modulated by this agent include transcription factors, growth factors and their receptors, cytokines, enzymes, and genes regulating cell proliferation and apoptosis [53]. The anti-carcinogenic properties of curcumin in animals have been demonstrated by its inhibition of tumor initiation [54] and tumor promotion [55, 56]. Studies of curcumin have shown that it influences structurally unrelated membrane proteins across several signaling pathways. [57] A recent report suggests that curcumin inserts deep into the cellular membrane in a transbilayer orientation, anchored by hydrogen bonding to the phosphate group of lipids, thus inducing negative curvature in the bilayer [58]. The promotion of negative curvature by curcumin may have a direct effect on apoptosis by increasing the permeabilizing activity of the apoptotic protein tBid. [59] Curcumin has been shown to suppress multiple signaling pathways and inhibit cell proliferation, invasion, metastasis, and angiogenesis. The chemo preventive action of curcumin might be due to its ability to induce apoptosis by several pathways. Curcumin directly or indirectly controls different gene or gene products involved in cell death pathways. [60] [Reviewed in 61]

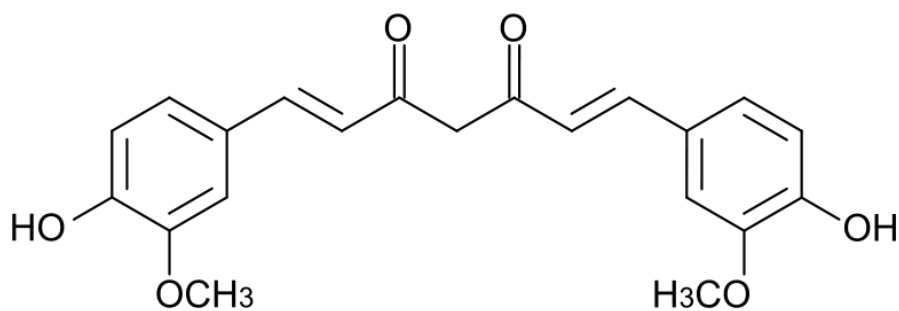


**Figure 3: Chemical structure of curcumin**

([http://www.avaplant.com/wp-content/uploads/2011/10/Curcumin\\_structure.png](http://www.avaplant.com/wp-content/uploads/2011/10/Curcumin_structure.png), 2017.07.04)

## 1.5 Apoptosis

The word apoptosis was published in the paper by Kerr, Wyllie, and Currie in 1972 for the first time. It is characterized by its especially morphological form of cell death and certain parts of this mechanism have been known and published many years ago. [62-64]

The mechanism of apoptosis is based on the process of programmed cell death that appears naturally during the development of the nematode *Caenorhabditis elegans*.

More than 1000 somatic cells in this creature are responsible for the formation of the adult worm, in which approximately 130 of these cells undergo programmed cell death which is known as apoptosis.

During the process of development, these 130 cells die at special points in the cell cycle, which is seen as an essential step in worms that shows us the exceeding exactness and control that needs to take place in this system. Programmed cell death has been admitted as an important and characteristic process in all living beings, which includes the elimination of special cells on the basis of genetics. [65] During the development and aging process the programmed cell death appears naturally, to preserve cell populations in tissues. It also functions as a protection mechanism, for example it takes places when cells get damaged by different chemicals or diseases, in order to prevent worse damage. [66] [Reviewed in 67]

### 1.5.1 Morphology of Apoptosis

Many different morphological changes take place in the cell during apoptosis that could be observed by using an electron and light microscope. [68] At the beginning of the process of programmed cell death, cells begin to shrink and the irreversible condensation of chromatin, which is known as pyknosis can be seen by light microscopy. This phase is characterised by the appearance of smaller cells, a cytoplasm that is more compact and the organelles in it are more tightly packed. But the most characteristic property in the process of apoptosis is definitively the condensation of the chromatin. [64] [Reviewed in 67]

## 1.5.2 Mechanisms of Apoptosis

The mechanisms that lead to the effect of apoptosis are based on a complex cascade of different molecular progresses that work together. Two main apoptotic pathways could be identified in the last years by many different groups of researchers which are better known as the extrinsic and the intrinsic pathway. The extrinsic pathways is also called the death receptor pathway and the intrinsic pathway is also known as the mitochondrial pathway. [69] Additionally a third pathway exists, which includes a perforin-granzyme dependent killing of the cells.

All of these three pathways come together and meet at a special point that continues with the execution pathway. The initiation of this pathway takes place by the cleavage of the caspase-3 and the end of the pathway leads to the fragmentation of DNA, degradation of different proteins, formation of apoptotic bodies and the expression of special ligands for death cell receptors. [Reviewed in 67]

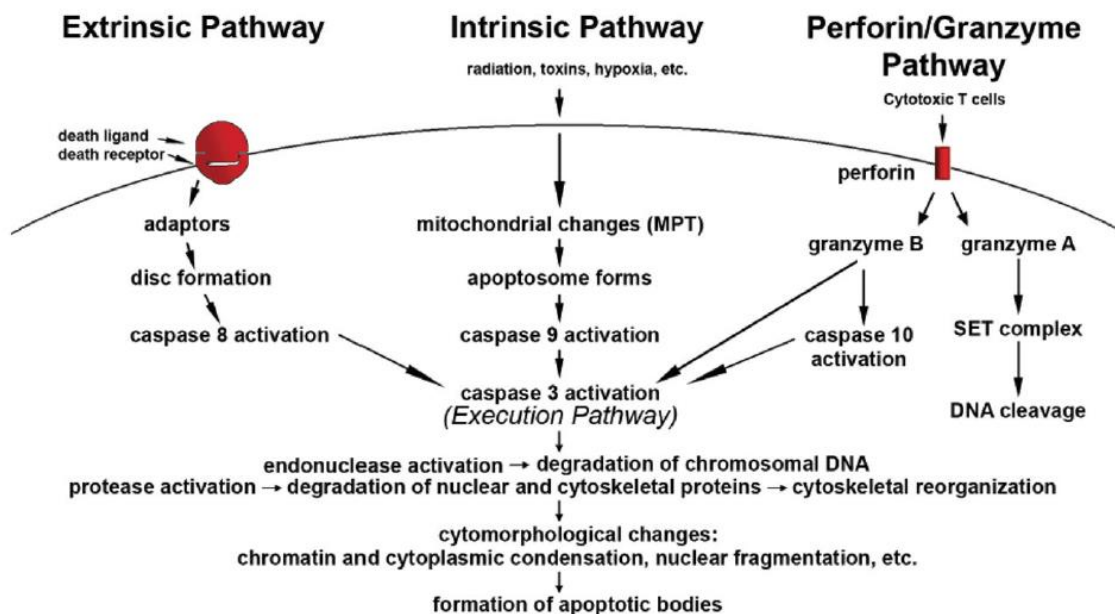


**Figure 4: Schematic representation of apoptotic events**

The two main pathways of apoptosis are extrinsic and intrinsic as well as a perforin-granzyme pathway. Each requires specific triggering signals to begin an energy-dependent cascade of molecular events. Each pathway activates its own initiator caspase (8, 9, and 10) which in turn will activate the executioner caspase-3. (Susan Elmore, Apoptosis: A Review of Programmed Cell Death, Toxicol Pathol. 2007 ; 35(4): 495–516)

### 1.5.3 Biochemical Features

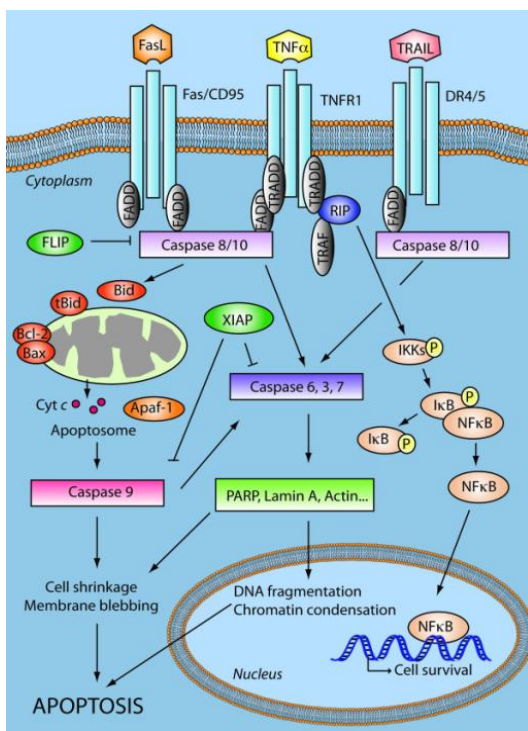
Many different biochemical modifications are present in apoptotic cells like the cleavage of proteins, the fragmentation of DNA, and the building of apoptotic bodies that lead to the special structural changes. [70]

In the most cells caspases are expressed in an inactive form, which can be activated by cleavage that again can be triggered by different external signals. The active form of them can activate other caspases leading to the initiation of a cascade of proteases. Aggregation and auto activation is an enzymatic feature of some caspases. This triggered cascade augments the apoptotic pathway and leads to the result of cell death. The proteolytic activity of caspases enables them to cleave proteins at aspartic acid residues, aside from the fact that different caspases have different efficacies. If caspases are once activated, this process cannot be reversed, which in the end leads to cell death. The existence of ten different major caspases have been observed, which were distributed into three different categories: First the initiator caspases (caspase-2,-8,-9,-10), second the effector caspases (caspase-3,-6,-7) and at least the inflammatory caspases (caspase-1,-4,-5). [71, 72]

The expression of cell surface markers has been observed to be another biochemical characteristic of apoptotic cells. The result of this feature is the recognition of apoptotic cells by neighbouring cells that enables the process of phagocytosis without harming the surrounding tissue. This step is characterised by the switching out of phosphatidylserine of the lipid bilayer of cells to the outer layer of the membrane that normally face inwards. [73] This switched phosphatidylserines on the surface of apoptotic cells are then recognized by phagocytes. Additionally to the movement of phosphatidylserine, other proteins were observed that were exposed on the cell surface during the process of apoptosis. One example would be the protein Annexin, which interacts with phosphatidylserine residues and thus can be used in the examination of apoptosis. [74] [Reviewed in 67]

### 1.5.4 Extrinsic Pathway

The extrinsic pathways of apoptosis is triggered by the binding of special ligands to transmembrane receptors. This membrane receptors are also called death receptors that belong to the tumor necrosis factor (TNF) receptor gene family. [75] All members of these receptor family share the same structural features such as similar cysteine-rich extracellular domains and they possess the so called “death domain”, a cytoplasmatic domain that is having the size of about 80 amino acids. [76] This death domain is responsible for the transmission of the death signal by binding of a ligand to the receptor to the intracellular pathway. Some of these ligands that bind to the death receptors are the Fas protein, the TNFR1 protein, the DR4 and the DR5 protein. [76-79] The extrinsic phase of apoptosis is well characterized and described by the Fas and TNFR1 models. A clustering of receptors takes place in this models, which is followed by the binding of the homologous trimeric ligand. After the binding of the ligands to the receptors adapter proteins are recruited possessing a death domain that binds the receptors. When the Fas ligand binds to the Fas receptor, the FADD adapter protein binds



to the cytoplasmatic part of the receptor and the binding of TNF ligand to the TNF receptor leads to the binding of the adapter protein TRADD. This results in the recruitment of FADD and RIP. [80, 81] Hence FADD interacts with procaspase-8/10 by the formation of a dimer. The formation of a death-inducing signaling complex (DISC) appears, and the auto-catalytic activation of procaspase-8/10 takes place. [82] The activation of this caspase is an irreversible step that results in the trigger of the execution phase of apoptosis. [Reviewed in 67]

**Figure 5: Extrinsic pathway of apoptosis**

The extrinsic pathway is activated by the binding of a ligand to a death receptors (TNFR1, Fas, DR4/5). This leads to the activation of a caspase cascade that results in the shrinkage of cells, the fragmentation of DNA and apoptosis. ([https://www.google.at/search?q=extrinsic+pathway+apoptosis&source=lnms&tbm=isch&sa=X&ved=0ahUKEwidgaKfy87VAhUEb1AKHeprAgkQ\\_AUICigB&biw=904&bih=423#imgrc=QvvXEz9dAwCotM](https://www.google.at/search?q=extrinsic+pathway+apoptosis&source=lnms&tbm=isch&sa=X&ved=0ahUKEwidgaKfy87VAhUEb1AKHeprAgkQ_AUICigB&biw=904&bih=423#imgrc=QvvXEz9dAwCotM))

### 1.5.5 Execution Pathway

Both the extrinsic and intrinsic pathway end at the same point of the execution pathway, which is also known as the final pathway of apoptosis. The start of this apoptotic phase is characterized by the activation of the execution caspases. Hence these execution caspases activate cytoplasmic endonucleases and proteases. The execution caspases lead to the degradation of nuclear material and the proteases result in the degradation of nuclear and cytoskeletal proteins. The effector caspases (caspase-3, caspase-6, and caspase-7) causes the cleavage of different substrates such as PARP, cytokeratins, the nuclear protein NuMA and others that are responsible for the structural and biochemical changes observed in apoptotic cells. [83] The most important of these executioner caspases is the caspase-3, which gets activated by any of the initiator caspases (caspase-8, caspase-9, or caspase-10). The endonuclease CAD, which causes degradation of chromosomal DNA and leads to chromatin condensation, is getting activated by caspase-3. In proliferating cells an inhibitor, ICAD, binds CAD, but in apoptotic cells ICAD is cleaved and CAD is released. [84] Cytoskeletal reorganization and degradation of the cell into apoptotic bodies is also induced by the active caspase-3. One of the key substrates of activated caspase-3 is gelsolin, which binds actin and functions as a nucleus for actin polymerization. Another function of gelsolin would be the binding of phosphatidylinositol biphosphate and signal transduction. Gelsolin is getting cleaved by caspase-3 and the cleaved fragments of gelsolin cleave actin filaments in a calcium independent manner. The result of this cleavage cascade is the disruption of the cytoskeleton, signal transduction and the intracellular transport. [85] The last component of apoptosis is the uptake of apoptotic cells. This phase is characterized by the asymmetry of the phospholipids and the switch-out of phosphatidylserine on the surface of apoptotic cell. The exact mechanism of the movement of the phosphatidylserine to the outer leaflet of the cell is not examined in detail, the assumption exists that the mechanism depends on the loss of aminophospholipid translocase activity. [77] Some research groups have observed that the regulation of phosphatidylserine movement on oxidatively stressed erythrocytes depends on the activity of Fas, caspase-8, and caspase-3. [86, 87] Non-inflammatory phagocytic recognition is supported by the appearance of phosphatidylserine on the outer leaflet of apoptotic cells, which leads to the early uptake of the cell. [88] [Reviewed in 67]

## 1.6 NF-kappa-B signaling pathway

NF-kappa-B (NF- $\kappa$ -B) is a pleiotropic transcription factor, which can be found in almost all cell types, and is the endpoint of a signal transduction cascade that gets initiated by a huge number of stimuli that are involved in many biological processes such as cell growth, differentiation, apoptosis and immune defence mechanisms. The NF- $\kappa$ -B complex can form either a homo- or a heterodimer and can be built up by the Rel-like proteins such as p50 (NF $\kappa$ B1), p65 (RELA), RELB, p105 (NF $\kappa$ B1), REL and p52 (NF $\kappa$ B2). The heterodimeric p65-p50 complex is the most common one. The NF- $\kappa$ -B sites in the nuclei are bound by the dimers and each dimer is having particular preferences for special NF- $\kappa$ -B sites that can be bound with different specificity and affinity. Depending on the combination of the dimer formation the different dimers can function either as transcriptional activators or repressors.

The different control mechanisms for the NF- $\kappa$ -B pathway involve post-translational modifications and interactions with other cofactors or co-repressors. The inactive form of the NF- $\kappa$ -B complexes are held in the cytoplasm by different members of the NF- $\kappa$ -B inhibitor (I $\kappa$ B) family. In a conventional activation pathway, the activation of I $\kappa$ B kinases like I $\kappa$ B- $\alpha$  results in the phosphorylation of the inhibitory I $\kappa$ B- $\alpha$  protein. NF- $\kappa$ -B is then released and translocates to the nucleus where it interacts with other transcription factors and transcriptional co-factors to regulate the expression of different genes. The NF- $\kappa$ -B heterodimeric p65-p50 complex functions as a transcriptional activators. The NF- $\kappa$ -B p65-p65 complex is involved in the invasin-mediated activation of IL-8 expression. [89] [90]

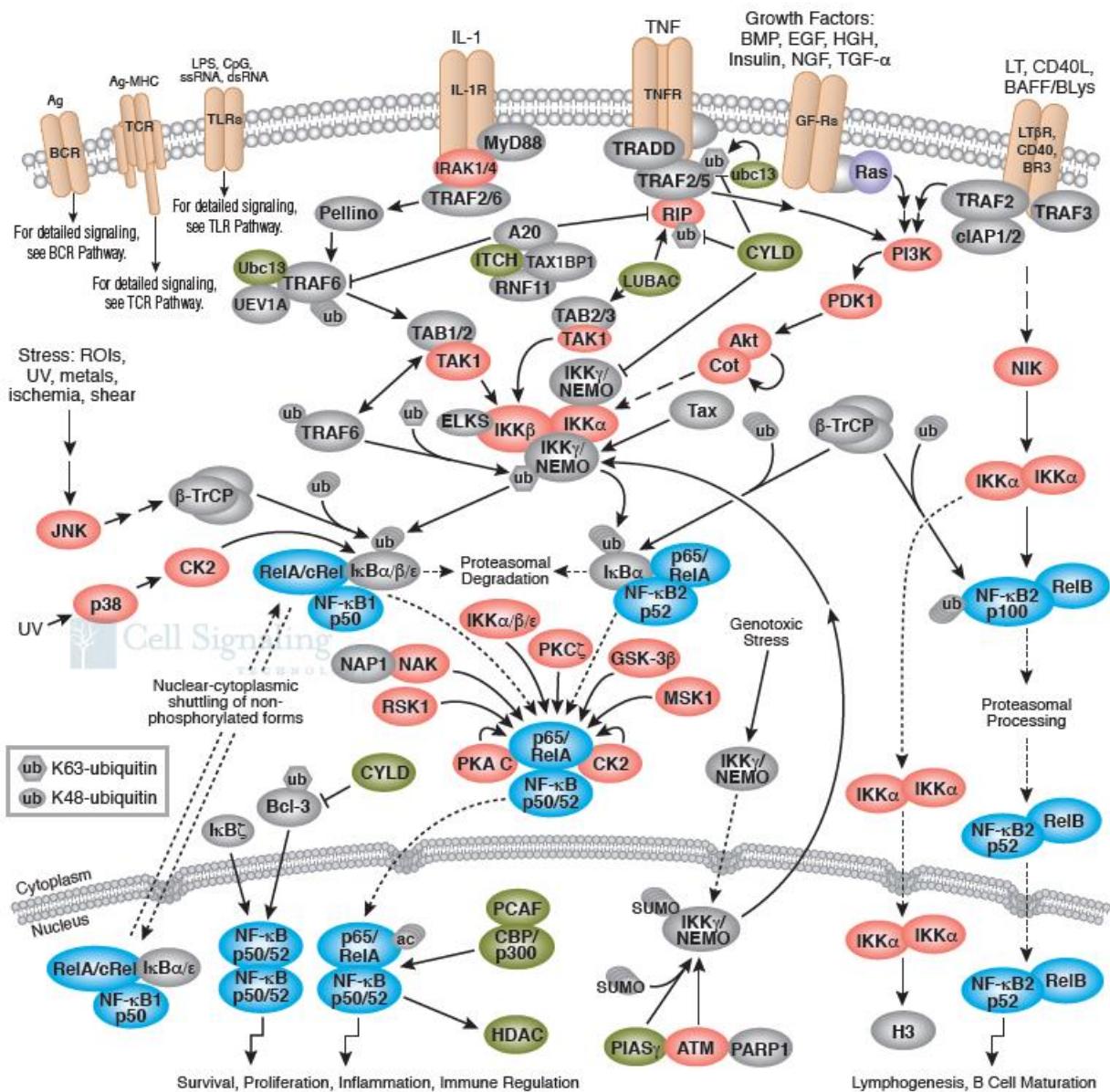


**Figure 6: NF-kappa-B signaling pathway.**

Nuclear factor- $\kappa$ B (NF- $\kappa$ B)/Rel proteins include RELA/p65, RELB, NFKB1/p105, NFKB1/p50, REL and NFKB2/p52 and the heterodimeric p65-p50 complex. These proteins function as dimeric transcription factors that regulate the expression of genes influencing a broad range of biological processes including innate and adaptive immunity, inflammation, stress responses, B-cell development, and lymphoid organogenesis. (<https://www.cellsignal.com/contents/science-pathway-research-immunology-and-inflammation/nf-b-signaling-pathway/pathways-nfkb>)

## 2 Methods

### 2.1 Cell culture

The synovial sarcoma cell line SW-982 (CLS, Eppelheim, Germany) and the OS cell line U2OS (ATCC, Manassas, VA) were cultured in Dulbecco's modified Eagle medium with DMEM-F12 (Gibco®, life technologies™, Carlsbad, USA), containing 10% fetal bovine serum (FBS) (Gibco®, life technologies™), 1% penicillin streptomycin (Gibco®, life technologies™), 1% l-glutamine (Gibco®, life technologies™) and 0.1 % amphotericin B (Sigma Aldrich, St. Louis, MO). The cells were cultured in a humidified atmosphere of 5% CO<sub>2</sub> at 37°C and the medium was changed every 3-4 days before cell density reached a confluence of approximately 95%.

### 2.2 Power Plex® system

Both cell lines were verified by short tandem repeat (STR) analysis. For the DNA isolation approximately  $5 \times 10^5$  cells were harvested by using accutase (Sigma Aldrich) and centrifuged (Megafuge 1.0 R, Heraeus, Hanau, Germany) at 300 x g for 4 minutes. The supernatant was discarded, the cell pellets were re-suspended with 200 µl PBS 1x (Gibco®, life technologies™) and the suspensions were transferred into 1.5 ml Eppendorf tubes. Then 20 µl Proteinase K were added to the samples. DNA preparation was performed by using QIAmp DNA Mini Kit (Qiagen, Hilden, Germany) and the manufacturer's protocol.

1. After adding 200 µl Buffer AL, the samples were mixed by vortexing for 15 s. In order to ensure efficient lysis, it is essential that the sample and Buffer AL were mixed thoroughly to yield a homogeneous solution.
2. Then the samples were incubated at 56°C for 10 min. DNA yield reached a maximum after lysis for 10 min at 56°C. Tubes were briefly centrifuged to remove drops from the inside of the lid.

3. Then 200  $\mu$ l 100% ethanol was added and the samples were mixed again by vortexing for 15 s. After mixing, the tubes were again briefly centrifuged to remove drops from the inside of the lid.
4. The mixtures were carefully applied to the QIAamp Spin Column (in a 2 ml collection tube) without wetting the rim. The cap was closed and the samples were centrifuged at 6000 x g (8000 rpm) for 1 min. The QIAamp Spin Column was placed in a clean 2 ml collection tube (provided) and the tube containing the filtrate was discarded.
5. The QIAamp Spin Columns were carefully opened and 500  $\mu$ l Buffer AW1 was added without wetting the rim. The cap was closed and centrifuged at 6000 x g (8000 rpm) for 1 min. The QIAamp Spin Columns were placed in a clean 2 ml collection tube (provided), and the collection tube containing the filtrate was discarded.
6. The QIAamp Spin Column was carefully opened and 500  $\mu$ l Buffer AW2 was added without wetting the rim. The cap was closed and centrifuged at full speed (20,000 x g; 14,000 rpm) for 3 min.
7. The QIAamp Spin Column was placed in a clean 1.5 ml micro centrifuge tube (not provided), and the collection tube containing the filtrate was discarded. The QIAamp Spin Column was carefully opened and 200  $\mu$ l Buffer AE was added. The samples were incubated at room temperature (15–25°C) for 1 min, and then centrifuged at 6000 x g (8000 rpm) for 1 min.
8. The QIAamp Spin Column was placed in a clean 1.5 ml tube and the collection tube with the filtrate was discarded.
9. The QIAamp Spin Column was carefully opened and 200  $\mu$ l Buffer AE was added. The samples were incubated at room temperature (15–25°C) for 1 min, and then centrifuged at 6000 x g (8000 rpm) for 1 min.

For the performance of the STR analysis the samples were sent to an external institute, where the Power Plex® 16 System (Promega, Vienna, Austria) was used.

### 2.3 Vimentin-DAPI Immunofluorescence staining

For the vimentin-DAPI immunofluorescence staining SW-982 and U2OS cells were seeded into chamber slides with  $3 \times 10^4$  cells/well. The cells were incubated for 2 days at 37°C until a confluence of 80% was reached. Then the cells were washed with 1 ml of PBS 1x (Gibco®, life technologies™) for three times, air dried for 2 hours at room temperature and stored at -20°C. Before starting to fix and stain the cells, all needed substances were prepared.

The vimentin antibody (Dako, Glostrup, Denmark) was diluted [1:100] with antibody diluent [1x PBS (Gibco®, life technologies™), 1% bovine serum albumin (Sigma Aldrich) and 0.3% Triton™ X-100 (Sigma Aldrich)]. The cy-2 conjugated goat anti-mouse antibody (Jackson ImmunoResearch, PA) was prepared in a solution at a ratio of 1:100 using the same antibody diluent. In the next step the cells were fixed using 4% formaldehyde (Promega, WI) for 10 minutes. Afterwards fixed cells were washed with PBS 1x (Gibco®, life technologies™). Afterwards the cells were blocked with UltraVision ProteinBlock (Thermo Fisher Scientific, Waltham, MA) for 5 minutes to reduce unspecific protein bindings for a better imaging quality with less background. Then 200 µl of the first diluted antibody, the vimentin antibody (Dako) was added into two of the chambers (Figure 7) and incubated for 30 minutes at room temperature. For negative control 200 µl of the diluted IgG [1:100] (Linaris, Dossenheim, Germany) was added to one chamber and 200 µl of the antibody-diluent without the first antibody was added to one chamber.

Vimentin -AB	Vimentin -AB	AB-diluent	IgG	
--------------	--------------	------------	-----	--

**Figure 7: The pipetting-layout of the vimentin-DAPI staining**

For negative control the diluted IgG was added to chamber 1 and the antibody-diluent without the first antibody was added to chamber 2. The diluted vimentin antibody was given to the chamber 3 and 4.

After 30 minutes of incubation and washing the cells three times for 5 minutes with PBS 1x (Gibco<sup>®</sup>, life technologies<sup>™</sup>), 200 µl of the cy-2 conjugated goat anti-mouse antibody (Jackson ImmunoResearch) was added to each chamber and incubated for 30 minutes at room temperature protected from light. This emerged complex could be visualized with a fluorescence microscope. After a second round of washing steps with PBS 1x (Gibco<sup>®</sup>, life technologies<sup>™</sup>) (3x5min), the stained sections were covered with Vectashield Mounting Medium (Dako) which contains 4', 6-diamidino-2-phenylindole (DAPI). DAPI binds to DNA rich regions and counterstained the nuclei, which led to a better orientation concerning the imaging and analysis. The cells were stored in the dark and viewed with a Confocal LSM 510 META Fluorescence Microscope (Zeiss, Vienna, Austria). ZEN 2009 software (Zeiss) was used to take and process the images.

## 2.4 Proliferation assay

### 2.4.1 Cell viability assay (MTS assay)

The MTS-Assay is a colorimetric method for determining the number of viable cells in proliferation assays based on the reduction (by dehydrogenase enzymes) of the tetrazolium salt, MTS ([3-(4,5-dimethylthiazol-2-yl)-5-(3-carboxymethoxyphenyl)-2-(4-sulfophenyl)-2H-tetrazolium]), to a coloured formazan compound by metabolically active mitochondria in viable cells in culture. Metabolism in viable cells produces "reducing equivalents" such as NADH or NADPH. These reducing compounds pass their electrons to an intermediate electron transfer reagent that can reduce MTS into the formazan product, which is soluble in cell culture medium. Upon cell death, cells rapidly lose the ability to reduce MTS into formazan. The production of the coloured formazan product is proportional to the number of viable cells in culture. [91] Tumor cells were adjusted to a density of  $3 \times 10^5$  cells/100 $\mu$ l and incubated for 24 h in 96-well microplates. The cells were exposed to various concentrations (0.19  $\mu$ M, 0.39  $\mu$ M, 0.78  $\mu$ M, 1.56  $\mu$ M, 3.125  $\mu$ M, 6.25  $\mu$ M, 12.5  $\mu$ M, 25  $\mu$ M, 50  $\mu$ M, and 100  $\mu$ M) of curcumin (Selleckchem, Houston, TX) 50 mg of curcumin were dissolved in 1 ml DMSO (Sigma Aldrich) to gain a concentration of 135.72 mM. A stock of 100  $\mu$ M was used to establish the concentrations named above for 24, 48 and 72 h, untreated cells were used for negative control, DMSO (Sigma Aldrich) was used for the positive control and culture medium was used for the blank. The drug sensitivity was determined by the MTS assay (Promega,) following the manufacturer's instructions using a photometer (Spektramax, BMG Labtech., Offenburg, Germany) at the wavelength of 490 nm.

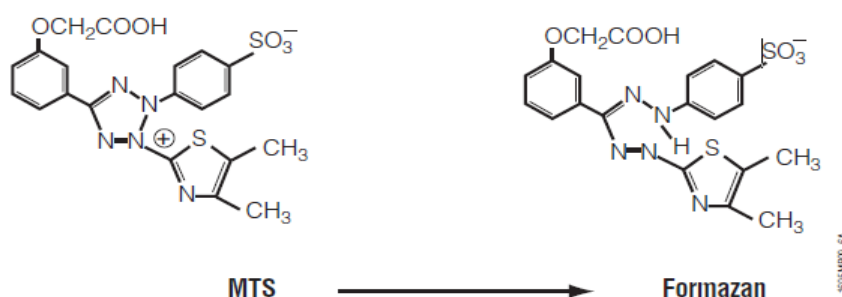


**Figure 8: Structures of MTS tetrazolium and its formazan product.** ([https://www.google.at/search?q=MTS+tetrazolium+and+its+formazan+product&source=lnms&tbm=isch&sa=X&ved=0ahUKEwj\\_s5eLzM7VAhUNaVAKHb79D7UQ\\_AUICigB&biw=904&bih=423#imgsrc=3n0QuMBbPz8woM](https://www.google.at/search?q=MTS+tetrazolium+and+its+formazan+product&source=lnms&tbm=isch&sa=X&ved=0ahUKEwj_s5eLzM7VAhUNaVAKHb79D7UQ_AUICigB&biw=904&bih=423#imgsrc=3n0QuMBbPz8woM))

## 2.4.2 xCELLigence Real-time cell analysis

The xCELLigence Real-time analysis system (OLS, Bremen, Germany) is based on a non-invasive impedance measurement that enables the quantification of adherent cell proliferation and viability in real time. A set of gold microelectrodes fused to the bottom surface of a microtiter plate well is the functional unit of the cellular impedance assay. When these gold microelectrodes are surrounded by an electrically conductive solution, the occurrence of an electric potential across these electrodes causes electrons to leave the negative terminal, pass through solution and then sediment onto the positive terminal to complete the circle. The presence of adherent cells at the electrode-solution interface impedes electron flow, because this phenomenon is dependent upon the electrodes interacting with solution. The magnitude of this impedance is dependent on the number of cells, the size and shape of the cells and the cell-substrate attachment quality. [92]

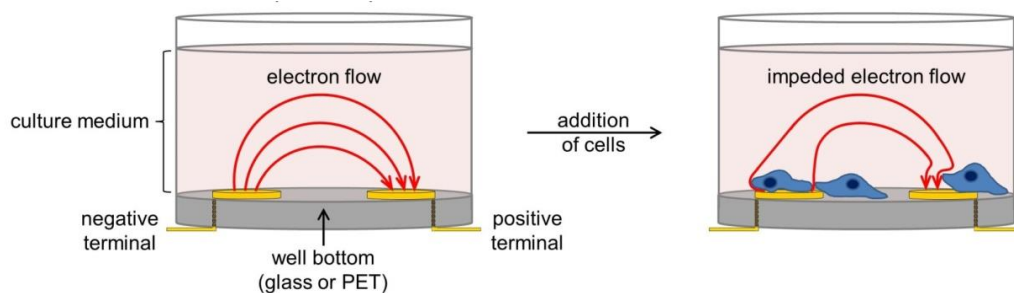


**Figure 9: Overview of cellular impedance apparatus.**

In the absence of cells electric current flows freely through culture medium, completing the circuit between the electrodes (left figure). As cells adhere to and proliferate on the electrodes current flow is impeded, providing an extremely sensitive readout of cell number, cell size/morphology, and cell-substrate attachment quality (right figure). (<https://www.aceabio.com/product/rtca-dp/>)

$3 \times 10^3$  cells were seeded in each of the 16-well micro plates (E-plates<sup>®</sup>, Roche Diagnostics, Rotkreuz, Switzerland), containing microelectronic sensor arrays. These sensors cover almost the whole area at the bottom of the 16-well microtiter plate. The culture medium serves as an electrically conductive solution and leads to the flow of electrons from the negative terminal to the positive terminal. The impedance that is generated by cells interacting with the sensors indicates the cell viability. This impedance was reported by the cell index (CI) that is dependent on the number as well as the size of cells.

## 2.5 Measurement of apoptosis by flow cytometry

### 2.5.1 Flow cytometer

Sheath fluid is used to focus the cell suspension through a small nozzle, when a cell suspension runs through the cytometer. The cells that are taken by a tiny stream of fluid pass a laser light one cell at a time. As they pass through the laser beam, the scattered light from the cells or particles is detected. The forward scatter (FS) is measured by a detector in front of the light beam and the side scatter (SS) is measured by several detectors to the side. Fluorescence detectors measure the fluorescence emitted from positively stained cells or particles. SS is proportional to the granularity of the cells and FS correlates with cell size. Because of this fact cell populations can often be distinguished based on differences in their granularity and size and alone. When the fluorescing cell pass the laser beam, it creates a peak or pulse of photon emission over time. These signals are detected by the PMT and converted to a voltage pulse, known as an event. The total pulse height and area is measured by the flow cytometer. The measured voltage pulse area will correlate directly to the intensity of fluorescence for that event. [93]

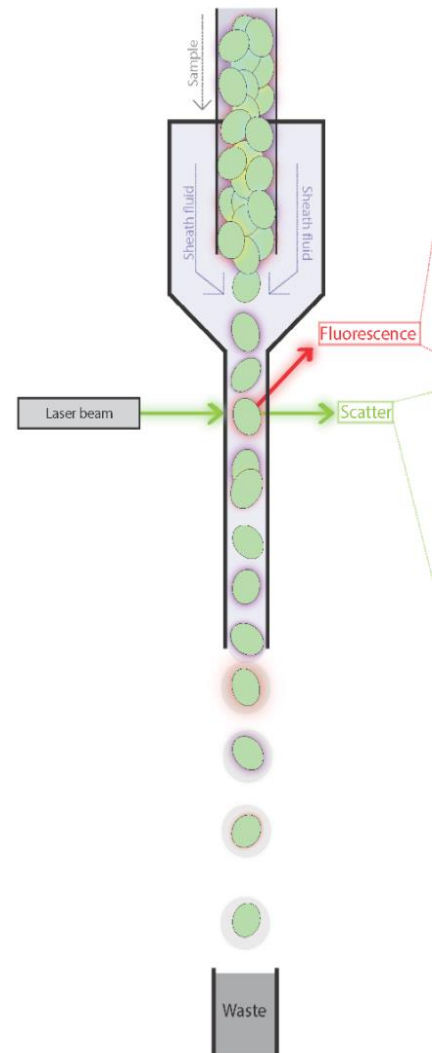


**Figure 10: Overview of the flow cytometer**

Sheath fluid focuses the cell suspension, causing cells to pass through a laser beam one cell at a time. Forward and side scattered light is detected, as well as fluorescence emitted from stained cells.

([http://docs.abcam.com/pdf/protocols/Introduction\\_to\\_flow\\_cytometry\\_May\\_10.pdf](http://docs.abcam.com/pdf/protocols/Introduction_to_flow_cytometry_May_10.pdf))

## 2.5.2 Cleaved caspase 3 assay

Apoptosis is a genetically programmed process that can be triggered through two different routes, the intrinsic and extrinsic pathway. Both are based on the proteolytic activity of caspases, which are expressed as inactive pro-enzymes that become activated upon proteolytic cleavage. Effector caspases such as caspase 3 cleave a large number of cellular proteins like major cytoplasmatic and nuclear elements, which form the biochemical basis of apoptotic cells. [94]

### Fixation

Cells were gained by centrifugation of the cell suspension and washed with PBS 1x (Gibco®, life technologies™). Carefully the cell pellet was re-suspended in 0.5 ml PBS and 4% formaldehyd (FA) was added till an end concentration of 2% FA was reached. The fixation step was performed at 37°C for 10 minutes and then the samples were kept on ice.

### Permeabilization

To the cell suspension 100% methanol was added slowly till an end concentration of 90% methanol was reached. The suspension was gently vortexed and incubated at 4°C for 30 minutes.

### Staining

The cell suspension was centrifuged, washed with incubation buffer and the pellet was re-suspended in incubation buffer [100 ml PBS (Gibco®, life technologies™) + 0.5 g BSA (Gibco®, life technologies™)]. The samples were incubated for 10 minutes at room temperature, 2 µl of the Alexa antibody (Cell Signaling, Alexa<sup>®</sup> 488, rabbit AK, Cambridge, United Kingdom) was added to each sample and incubated for 30 – 60 minutes at room temperature in the dark. After centrifugation the cell pellet was re-suspended in PBS 1x (Gibco®, life technologies), transferred into micronics and measured by using the FACS LSR II System (BD Bioscience, San Jose, CA). Data were acquired and analysed by using FACSDiva™ software (BD Bioscience).

### 2.5.3 Annexin/PI assay

Annexin V is a member of the annexin family of intracellular proteins that binds to phosphatidylserine (PS) in a calcium-dependent manner. PS normally is only found on the intracellular leaflet of the plasma membrane in healthy cells, but during early apoptosis, membrane asymmetry is lost and PS translocates to the external leaflet. Fluorochrome - labelled Annexin V can then be used to specifically target and identify apoptotic cells and cells that are Annexin V<sup>+</sup>/PI<sup>-</sup> represent early apoptotic cells. Annexin V binding alone cannot differentiate between apoptotic and necrotic cells. To help distinguish between the necrotic and apoptotic cells propidium iodide (PI) was used. Early apoptotic cells will exclude PI, while late stage apoptotic cells will stain positively, due to the passage of this dye into the nucleus where it binds to DNA. [95]

The APC Annexin V Apoptosis Detection Kit (BioLegends, San Diego, CA) was performed following the manufacturers' instructions. Apoptotic cells were identified by the incubation of  $1 \times 10^6$  cells in 100  $\mu$ L Annexin V Binding buffer containing 5  $\mu$ L Annexin V-APC and 5  $\mu$ L PI for 15 min at room temperature. Untreated cells were used as negative control. The apoptotic cells were determined using the FACS LSR II System (BD Bioscience), data were acquired and analysed by using FACSDiva<sup>TM</sup> software (BD Bioscience). Viable cells were gated on forward scatter (FSC) and side scatter (SSC) in order to exclude debris and cell aggregates.

## 2.6 Quantitative Real-time Polymerase Chain Reaction

Quantitative Real-time Polymerase Chain Reaction (qPCR) was performed to examine the relative expression of the FAS-associated death domain gene (FADD), the Fas cell surface death receptor gene (FAS), the death receptor 4 gene (DR4) and the tumor necrosis factor receptor 1 gene (TNFR1) with untreated and treated (curcumin) SW-982 and U2OS cells.

### 2.6.1 RNA isolation

RNA was isolated from the SW-982 and U2OS cell lines that were treated with curcumin (Selleckchem) before. For the negative sample the cells were treated with culture medium with the RNeasy Mini Kit (Qiagen, Hilden, Germany) and the RNA isolation was performed using the manufacturer's protocol.

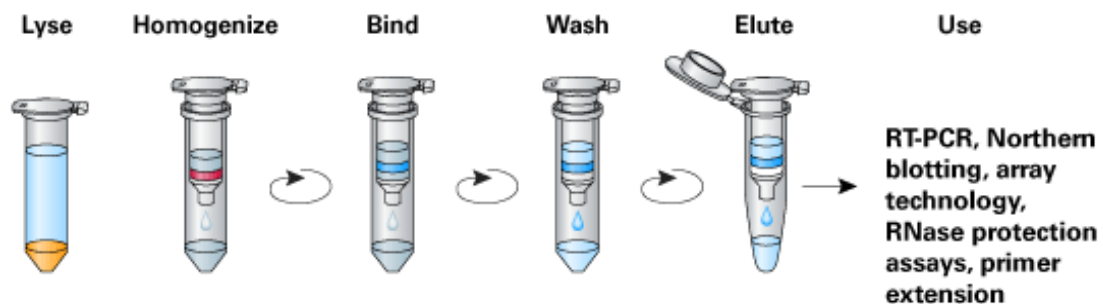


**Figure 11: Steps of RNA isolation**

([http://www.clontech.com/US/Support/Applications/Nucleic\\_Acid\\_Purification/Total\\_RNA\\_Purification?sitex=10020:22372](http://www.clontech.com/US/Support/Applications/Nucleic_Acid_Purification/Total_RNA_Purification?sitex=10020:22372):US)

1. For the RNA isolation approximately  $5 \times 10^6$  cells were harvested by using accutase (Sigma Aldrich) and centrifuged (Megafuge 1.0 R, Heraeus) at  $300 \times g$  for 4 minutes. The supernatant was discarded, the cell pellet was re-suspended with  $200 \mu\text{l}$  PBS 1x (Gibco®, life technologies™) and the suspensions were transferred into 1.5 ml Eppendorf tubes. The tubes were centrifuged at  $300 \times g$  for 5 min and the supernatant was completely aspirated.
2. The cells were disrupted by adding Buffer RLT. Then the appropriate volume of Buffer RLT was added and the samples were vortexed.

3. The lysate was pipetted directly into a QIAshredder spin column placed in a 2 ml collection tube, and centrifuged for 2 min at full speed.
4. 1 volume of 70% ethanol was added to the homogenized lysate, and mixed well by pipetting.
5. Up to 700  $\mu$ l of the sample was transfer, including any precipitate that may have formed, to an RNeasy spin column placed in a 2 ml collection tube. The lid was gently closed and centrifuged for 15 s at 8000 x g. The flow-through was discarded.
6. 700  $\mu$ l Buffer RW1 was added to the RNeasy spin column, the lid was gently closed and centrifuged for 15 s at  $\geq$ 8000 x g to wash the spin column membrane. The flow-through was discarded.
7. 500  $\mu$ l Buffer RPE was added to the RNeasy spin column. The lid was gently closed, and centrifuged for 15 s at  $\geq$ 8000 x g to wash the spin column membrane. The flow-through was discarded.
8. 500  $\mu$ l Buffer RPE was added to the RNeasy spin column. The lid was gently closed, and centrifuged for 15 s at  $\geq$ 8000 x g to wash the spin column membrane.
9. The RNeasy spin column was placed in a new 1.5 ml collection tube and 30–50  $\mu$ l RNase-free water was added directly to the spin column membrane. The lid was gently closed, and centrifuged for 1 min at  $\geq$ 8000 x g to eluate the RNA.

The total RNA concentration of the samples was quantified by using the NanoDrop spectrometer (Thermo Fisher Scientific, Waltham, MA). The measurement was performed by using 2  $\mu$ l of each sample. This measurement technique is based on the Lambert–Beer law, where the absorbance of the samples changes linearly with the concentration. RNA is having its absorbance maximum at 260 nm and proteins or other contaminations have their absorbance maximum at 280 nm. By using the ration of 260 nm and 280 nm absorbance the RNA purity was examined. Ratios between 1.8 and 2.0 predict pure and uncontaminated RNA.

## 2.6.2 Removal of genomic DNA and cDNA synthesis

For removing the genomic DNA the DNase, RNA- free I kit (Thermo Fisher Scientific) was used. Therefore 1  $\mu$ l RNA of each sample was purified with DNase and afterwards reverse-transcribed into cDNA by using the iScript cDNA Synthesis Kit (Bio-Rad Laboratories, Hercules, CA) using the manufacturer's protocol.

### Removal of genomic DNA (Thermo Scientific #EN0521):

RNA 1 $\mu$ g (add up to 8 $\mu$ l)	x $\mu$ l
10x reaction buffer with MgCl <sub>2</sub>	1 $\mu$ l
DNase I, RNase-free	1 $\mu$ l
Diethylpyrocarbonate (DEPC)-treated water	<u>x <math>\mu</math>l</u>
	<u>10 <math>\mu</math>l</u>

The substances, named above, were mixed together and incubated for 30 minutes at 37°C. After adding 50 mM ethylenediaminetetraacetic acid (EDTA) to each sample the samples were incubated for 10 minutes at 65°C.

### cDNA synthesis with the iScript cDNA Synthesis Kit(Bio-Rad, #170-8891, 100rxn):

5x iScript reaction mix	4 $\mu$ l
iScript reverse transcriptase	1 $\mu$ l
nuclease-free water (NFW)	4 $\mu$ l
RNA template	<u>11 <math>\mu</math>l</u>
	<u>20 <math>\mu</math>l</u>

Thermocycler reaction protocol:

5 min	25°C
30 min	42°C
5 min	85°C
Hold at	4°C

The substances were mixed together and incubated by using the thermocycler reaction protocol named above.

### 2.6.3 Real-time – quantitative Polymerase Chain Reaction

qPCR protocol:

Sso Advanced™ universal SYBR® Green supermix 2x	15µl
Quantitect Primer 10x	3µl
NFW	9µl
Template (12.5ng)	<u>3 µl</u>
	<u>60µl</u>

The substances named above were mixed together, vortexed and spinned in a centrifuge. After that 3x 10 µl of each sample was pipetted in a single well of a 96-well plate. The plate was sealed with optical film (APPLERA Biosystems, Vienna, Austria) and centrifuged for 2 minutes at 230 x g to get all liquids to the bottom of the wells. RT-PCR amplification was started with a 2 min step at 50°C, followed by a 3 min step at 95°C and 40 cycles of 15 sec at 95°C, and 1 min at 60°C by using the Bio-Rad CFX96. Relative quantification was based on internal reference gene GAPDH to determine fold-differences in expression of the target gene.  $\Delta\Delta CT$ - method was used for analysis taking the control as second reference.

## 2.7 Proteome profiler array (NFκB-assay)

Carefully selected capture antibodies have been spotted in duplicate on nitrocellulose membranes. Cell lysates were diluted and mixed with a cocktail of biotinylated detection antibodies. The mixture was then incubated with the array. Any protein/detection antibody complex present was bound by its capture antibody on the membrane. Streptavidin-Horseradish Peroxidase and chemiluminescent detection reagents were added for detection. [96]

1.  $1 \times 10^7$  cells were seeded for this array and washed with PBS 1x, making sure to remove any remaining PBS before adding lysis buffer. Cells were solubilised in 1 ml Lysis Buffer 6. The samples were up and down pipetted to re-suspend them and the lysates were gently rocked at 2-8°C for 30 minutes. After microcentrifugation at 14,000 x g for 5 minutes, the supernatant was transferred into a clean test tube.
2. 2.0 mL of Array Buffer 3/6 was pipetted into each well of the 4-Well Multi-dish to be used. Array Buffer 3/6 served as a blocking buffer.
3. By using flat-tip tweezers, each membrane was removed to be used from between the protective sheets and placed in a well of the 4-Well Multi-dish. The array number was facing upwards.
4. The membranes were incubated for one hour on a rocking platform shaker.
5. While the membranes were blocking, samples were prepared by adding the desired quantity of lysate to Array Buffer 1 for a total volume of 1.5 ml.
6. Array Buffer 3/6 was aspirated from the wells of the 4-Well Multi-dish. The prepared samples were added and the lid was placed on the 4-Well Multi-dish.
7. The membranes were incubated overnight at 2-8°C on a rocking platform.

8. Each membrane was carefully removed and placed into individual plastic containers with 20 ml of 1X Wash Buffer. The 4-Well Multi-dish was rinsed with distilled water and was dried thoroughly.
9. Each membrane was washed with 1X Wash Buffer for 10 minutes on a rocking platform shaker. This step was repeated two times for a total of three washes.
10. For each array, 15  $\mu$ l of reconstituted Detection Antibody Cocktail was diluted to 1.5 ml with Array Buffer 3/6. 1.5 ml per well of diluted Detection Antibody Cocktail was pipetted into the 4-Well Multi-dish.
11. Each membrane was carefully removed from its wash container. Excess buffer drained from the membrane and the membrane was returned to the 4-Well Multi-dish containing the diluted Detection Antibody Cocktail. The wells were covered with the lid.
12. The membranes were incubated for 1 hour at room temperature on a rocking platform shaker.
13. Each array was washed as described in steps 8 and 9.
14. The Streptavidin-HRP was diluted in Array Buffer 3/6 using the dilution factor on the vial label. 2.0 ml was pipetted into each well of the 4-Well Multi-dish.
15. Each membrane was carefully removed from the wash container. Excess Wash Buffer drained from the membrane. The array was returned to the 4-Well Multi-dish containing the diluted Streptavidin-HRP, and it was covered with the lid. The membranes were incubated for 30 minutes on a rocking platform shaker.
16. Each array was washed as described in steps 8 and 9.

17. Each membrane was carefully removed from its wash container. Excess Wash Buffer drained from the membrane by blotting the lower edge onto paper towels. Each membrane was placed on the bottom sheet of the plastic sheet protector with the identification number facing up.
18. 1 ml of the prepared Chemi Reagent Mix was pipetted onto each membrane.
19. Each membrane was carefully covered with the top sheet of the plastic sheet protector. The membrane was incubated for 1 minute.
20. Paper towels were positioned on the top and sides of the plastic sheet protector containing the membranes and Chemi Reagent.
21. The top plastic sheet protector was removed and an absorbent lab wipe was carefully laid on top of the membranes to blot off any remaining Chemi Reagent Mix.
22. Leaving membranes on the bottom plastic sheet protector, the membranes were covered with plastic wrap taking care to gently smooth out any air bubbles. The excess plastic wrap was wrapped around the back of the sheet protector so that the membranes and sheet protector were completely wrapped.
23. The membranes were incubated with 3 ml reagent (reagent A and B mixed in 1:1 ration) (ECL system, GE Healthcare, Illinois, USA) for 3-5 minutes without agitation placed with the identification numbers facing up in the ChemiDocTouch (Biorad).
24. The membranes were exposed for 1-10 minutes. Multiple exposure times were recommended.

## 2.8 Western Blot

### 2.8.1 Gel casting

Polyacrylamide gels are crosslinked, inert structures, in which the pore sizes in these gels are similar to the molecular radius of many proteins. An electric field is created, where molecules get forced in the gel. Larger molecules are retarded by the gel more than smaller molecules. The protein separating technique is based on the standard means of the molecular weight of proteins. The polymerization of the two compounds acrylamide and Bis-acrylamide is the most important step in the formation of polyacrylamide gels. Bis is a cross-linking agent for the gels. By the addition of ammonium persulfate along with TEMED the polymerization is initiated. The gels are three-dimensional networks that appear hydrophilic and neutral. The network is built up by long hydrocarbons, which are crosslinked by methylene groups. The relative size of the pores that are formed in the gel are responsible for the grade of separation of the molecules within the gel. The pore size of a gel depends on two factors: the amount of cross-linkers and the total amount of acrylamide that is present. As the percentage of acrylamide increases, the pore size decreases. Polyacrylamide is used to separate most proteins, ranging in molecular weight from  $M_r >5000$  to  $<200\,000$ . [97]

<u>% Gels</u>	<u>size of the protein to be determined</u>
15%	15 - 45 kDa
12.5%	15 - 60 kDa
10%	18 - 75 kDa
7.5%	30 - 120 kDa
5%	60 - 212 kDa

**Table 1: Recommended acrylamide concentration for protein target within defined size ranges**

The percentage of polyacrylamide used in the gel along with the buffer system will influence the mobility of the proteins through the gel as current is applied. The expected size of the target protein can be used to select the best gel/buffer system to achieve optimal separation and resolution.

## 2.8.2 Preparation for the gel casting

Plates needed to be cleaned with double distilled water and ethanol before usage, because contaminations can interrupt the polymerization or the electrophoresis of the gel. One spacer plate and one short plate were put together that the edges were coincided and both together were put into a gel caster.

<b>1-2 x Lower Gel</b>	<b>%-Gel</b>	<b>10</b>	<b>15</b>
	Volume [ml]	20	20
	DDI H <sub>2</sub> O	9.8	7.3
	40% Acrylamide [ml]	5	7.5
	Tris 1.5M [ml]	5	5
	10% SDS [ml]	0.2	0.2
	APS 10% [ml]	0.15	0.15
	TEMED [ml]	0.015	0.015
	Solution was mixed, gels were casted immediately and overlaid with H <sub>2</sub> O		
<b>8 x Upper Gel</b>	<b>%-Gel</b>	<b>3</b>	
	Volume [ml]	15	
	DDI H <sub>2</sub> O	9.975	
	40% Acrylamide [ml]	1.123	
	Tris 1.5M [ml]	3.75	
	10% SDS [ml]	0.15	
	APS 10% [ml]	0.15	
	TEMED [ml]	0.03	
	Solution was mixed, gels were casted immediately and overlaid with H <sub>2</sub> O		

**Table 2: Recipes of gels**

Reference recipe of 3% stacking gel and reference recipe of 20 ml separating gel in 10% and 15%.

### Pouring lower gels

1. Lower gels were prepared with the protocol above. APS and TEMED were added at the very end and the gels were poured into the gel caster.
2. Lower gel was overlaid with ddH<sub>2</sub>O, to avoid desiccation and gels polymerized for 45-60 min at room temperature.

### Pouring upper gels

1. Water was titrated and upper gels were prepared with the protocol above. APS and TEMED were added at the very end and the gels were poured into the gel caster.
2. Combs were slowly put in to avoid the appearance of air bubbles and gels polymerized for 30-45 min at room temperature.

## 2.8.3 Sample preparation and gel electrophoresis

### Protein extraction

The cell culture dishes were placed in ice and the supernatant was transferred into a Falcon tube. Cells were washed with cold PBS 1x and the supernatant was transferred into the same Falcon tube than before. The Falcon tubes were centrifuged at 1300xg for 5 min. The supernatant was discarded and the pellets were washed with PBS 1x. The PBS was drained, and then ice-cold lysis buffer was added, which includes protease inhibitors to prevent degradation of proteins following the release of endogenous proteases during the process of cell lysis. When lysis starts to begin, also dephosphorylation, denaturation and proteolysis appear. If samples are kept on ice the whole time and special inhibitors are added freshly to the lysis buffer, these events can be slowed down. Adherent cells were scraped off the dish by using a cold plastic cell scraper, then the cell suspensions were gently transferred into a pre-cooled Eppendorf tube. The pellet from the Falcon tubes was re-suspended with its belonging cell suspension and the samples were maintained at constant agitation for 10 minutes at 4°C. Then the samples were centrifuged at 16000x g for 20 minutes in a 4°C pre-

cooled micro centrifuge (Centrifuge 5415R, Eppendorf, Hamburg, Germany). The tubes were gently removed from the microcentrifuge and placed on ice. The supernatant was transferred to a fresh tube kept on ice and the pellet was discarded.

### Protein quantification

After the extraction of proteins from cells, the protein samples had to be quantified, that it was possible to compare the samples in different lanes within the same gel. To achieve this, the same amount of protein from each sample had been loaded on the gel. To determine the concentration of the proteins the Pierce BCA Protein Assay Kit (Thermo Scientific #23227) was used to perform a BCA.

The Thermo Scientific™Pierce™BCA Protein Assay is a technique used for the colorimetric detection and quantification of total protein. It is a detergent-compatible formulation based on bicinchoninic acid (BCA). This method is based on the reduction of  $\text{Cu}^{+2}$  to  $\text{Cu}^{+1}$  by proteins in an alkaline medium and the highly sensitive and selective colorimetric detection of the  $\text{Cu}^{+1}$  using a special reagent that contains bicinchoninic acid. Two molecules of BCA and one  $\text{Cu}^{+1}$  ion form a chelation that is having a purple colour, which is the basis of this assay. This complex is having its absorbance maximum at 562nm that is nearly linear with increasing protein concentrations over a broad working range.

1. A set of protein standards was prepared by using different dilutions of one Albumin Standard (BSA) ampule as it was described in table 3.
2. The BSA working reagent was prepared by mixing 7 ml of reagent A and 140  $\mu\text{l}$  of reagent B. For each well 200  $\mu\text{l}$  of the BSA working reagent was needed. [(number of samples in triplicates + number of standards in duplicates) x 200]
3. 25  $\mu\text{l}$  of each standard (2x) or 25  $\mu\text{l}$  of the sample (3x) was pipetted into a well of a 96-well plate.
4. 200  $\mu\text{l}$  of the working reagent was added and mixed gently.

The samples were incubated for 30 min at 37°C in the dark and measured at 562 nm at the Spectrostar (bmglabtech, Ortenberg, Germany).

Vial	Volume of Diluent $\mu\text{l}$	Volume of Albumin Stock 2000 $\mu\text{g/ml}$	Final BCA Concentration $\mu\text{g/ml}$
A	0	300 of Albumin Stock	2000
B	125	375 of Albumin Stock	1500
C	325	325 of Albumin Stock	1000
D	175	175 of B	750
E	325	325 of C	500
F	325	325 of E	250
G	325	325 of F	125
H	400	100 of G	25
I	400	0	0 = Blank

**Table 3: Volume list for the preparation of different albumin standard dilutions**

The protein samples were diluted with double distilled water to an end concentration of 20-40  $\mu\text{g}$  protein and 15  $\mu\text{l}$  of Laemmli Buffer was added to each sample. The tubes were vortexed, shortly centrifuged and put on the heating block (Eppendorf) for 5 min at 95°C to denaturate them. The combs are gently pulled out of the gel and the slots were washed with running buffer. The samples were pipetted into the wells and the gel was runned for one hour at 150V.

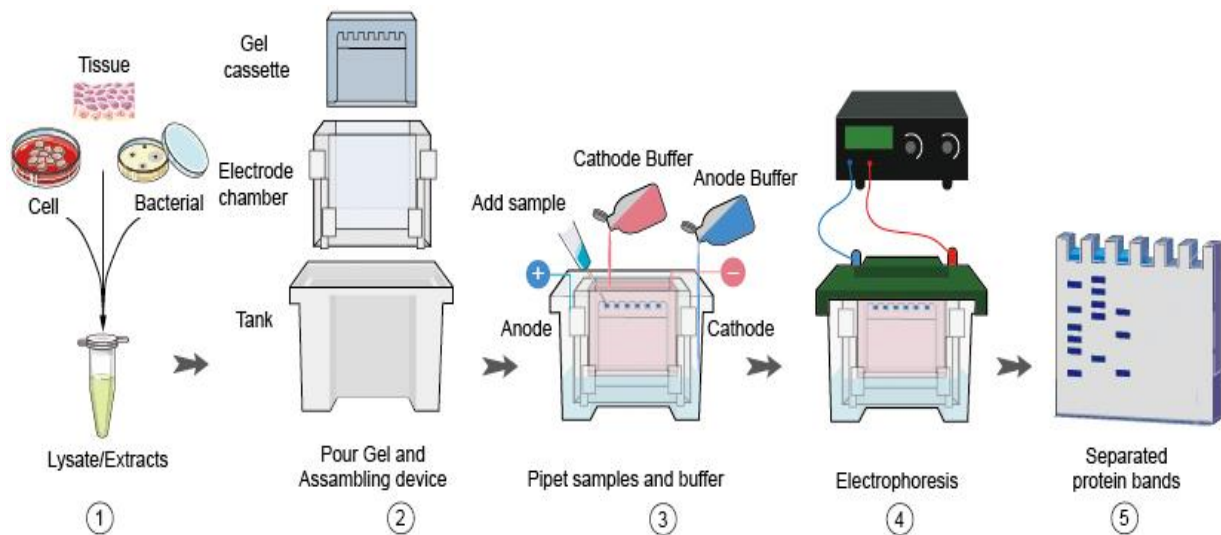


**Figure 12: Experimental steps of western blotting from sample preparation to protein electrophoresis.**  
 (<http://www.creative-diagnostics.com/Sample-Gel-Preparation.htm>)

#### 2.8.4 Protein transfer

After completion of the separation of proteins by polyacrylamide gel electrophoresis, the next step was the transfer of the proteins from the gel to a solid support membrane for further analysis. This membrane is usually made of nitrocellulose (NC) or polyvinylidene fluoride (PVDF). In this choice of transfer, the gel and membrane are both fully immersed in transfer buffer and a current is applied in the direction of the gel to the membrane. Generally, wet transfer requires cooling of the unit and internal recirculation of the transfer buffer by the presence of a stirring magnet.

### Protocol of wet transfer

- 1) The stacking gel was cut away and one corner was cut from the resolving gel, that enabled the correct orientation of the gel if it “flips over” during equilibration.
- 2) The membrane was pre-wetted and equilibrated in transfer buffer.
- 3) A sponge was pre-wetted and placed on the submerged part of the cassette. All air bubbles were removed by gently pressing. Two pre-wetted blotting papers were placed onto the sponge. The membrane was placed on top of the blotting papers. The gel was placed on top of the membrane. Two additional pre-wetted blotting papers were placed on the gel. All air bubbles were removed by gently pressing. Finally a pre-wetted sponge was placed on top of the stack and the cassette was closed.
- 4) The cassette was placed in the transfer tank (Important to watch out the orientation). The membrane should be closest to the anode (+) as the protein with negative charge would move towards the anode.
- 5) The transfer tank was connected to the power supply and transferred at 100V for 1h.

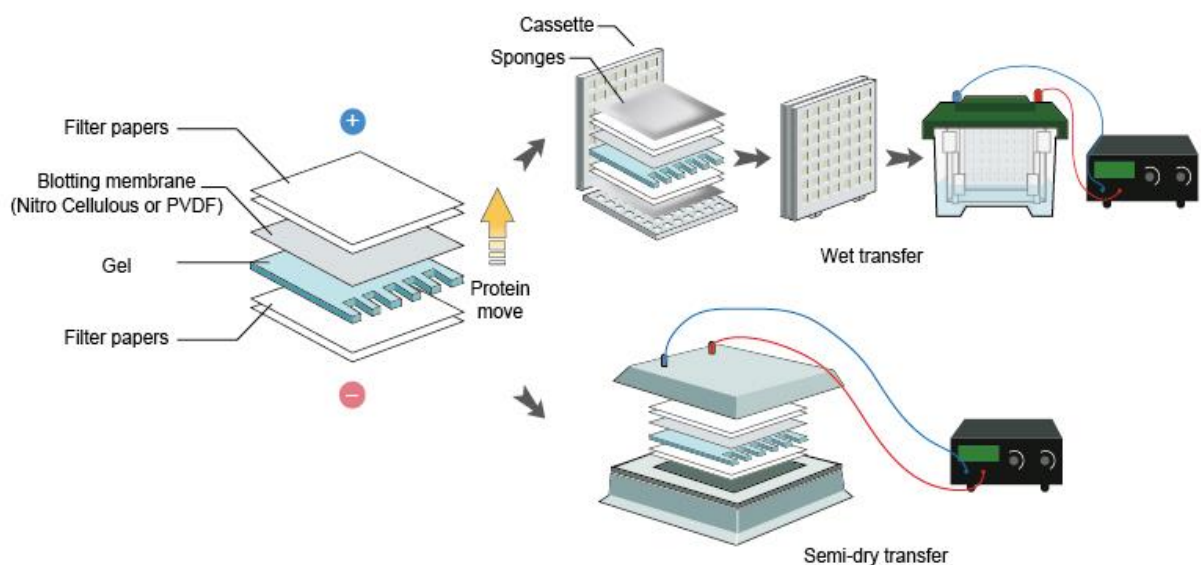


**Figure 13: Two electro-transfer techniques: the wet transfer and the semi-dry transfer.**

(<http://www.plagscan.com/highlight?doc=115130402&source=54&hl=textonly#1>)

### Blocking

The successfully on the membrane transferred proteins were stained with Ponceau S dye (Merck, Darmstadt, Germany). The membranes were incubated in Ponceau S for 5 minutes and washed with water until the bands were clear. After verification, the bands could then be de-stained by continuing to wash with water or TTBS 1x [TTBS 10x: 63.04g TRIZMA Hydrochloride (Sigma), 160.12g NaCl (Sigma), 20ml Tween 20 (Merck) and 2000 ml A.D] until the dye is completely removed. As non-specific binding of antibodies to the membrane is detrimental to the specificity and sensitivity of the assay, it is essential to "block" spaces not already occupied by proteins. The membranes were blocked with 3% milk buffer (completa) for 2 hours at room temperature and washed three times with TTBS 1x for 10 minutes.

### Primary antibody incubation

Following the blocking step, the protein of interest can be detected using antibodies. The primary antibody was diluted in a blocking buffer at the concentration recommended to the datasheet. The membranes were incubated overnight at 4°C with gentle shaking. The next day, the primary antibody solution was decanted off and the membrane was washed with large volumes of TTBS 1x. These stringent washes are extremely important for removing non-specific background signals.

### Secondary antibody incubation

The choice of secondary antibody depends on the species in which the primary antibody was produced. For example, the primary antibody was of the IgG isotype and produced in goat, the secondary antibody must be an anti-goat IgG antibody produced in another species as it will bind to the Fc region of the primary antibody. Although there is no strict rule, secondary antibodies raised in certain host species may lead to high background levels. The procedures for incubation of the secondary antibody solution and the membrane were similar to those described for the primary antibody. The secondary antibody was diluted in blocking buffer and the membrane was incubated for 1h at room temperature at the concentration recommended

on the data sheet. The secondary antibody was decanted and the membrane was washed with large volume of TTBS 1x.

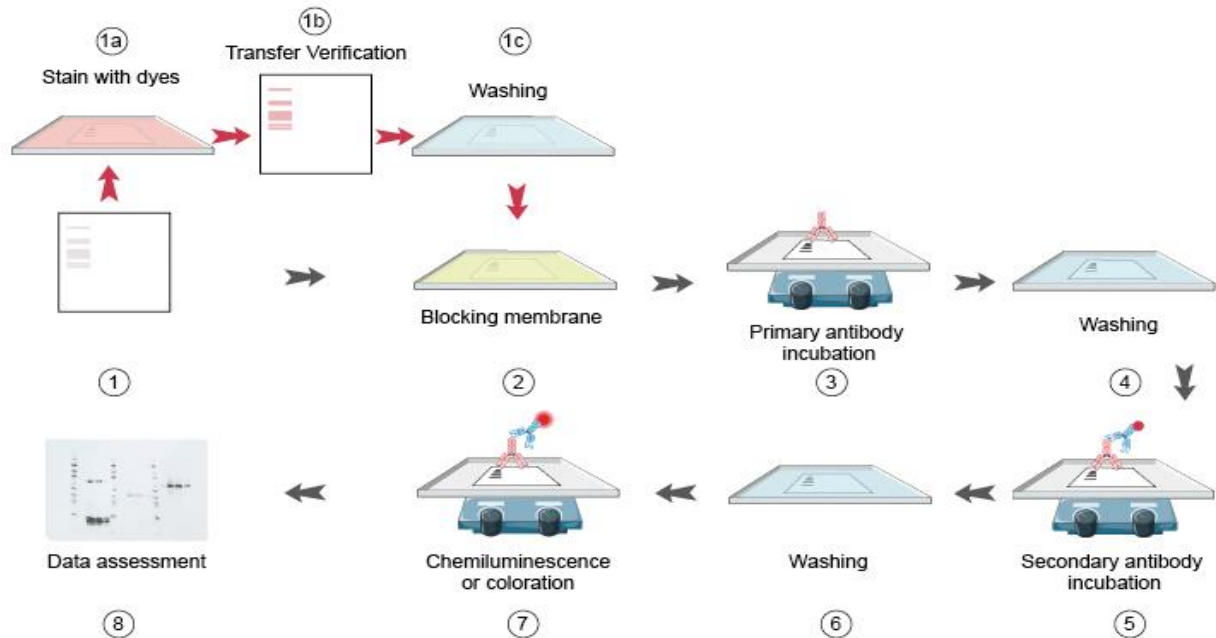


**Figure 14: The antibody incubation process of western blotting after protein transfer onto the membrane.**  
<http://www.creative-diagnostics.com/Antibody-Incubation-Gel-Visualization.htm>

### Visualization

A variety of detection systems, based on chemiluminescence, chemifluorescence, fluorescence, chromogenic or radioisotopic detection are available.

The most common, most sensitive and most inexpensive detection method is the electrochemiluminescence (ECL) system (GE Healthcare, IL). This method utilizes the HRP enzyme, which was conjugated to the secondary antibody to catalyse the ECL reaction and produce light. The light is then gathered by detection machine and digitized by using a specialized CCD camera that is sensitive enough for detection. There are two kinds of ECL reagents: reagent A and reagent B. These two ECL reagents were mixed in 1:1 ratio and the membrane was incubated into 3 ml reagent for 3-5 minutes without agitation. After incubation, the ECL mixture was decanted and a wipe was used to wipe off excess solution from the corner of the membrane. The membrane was placed in a clear plastic wrap such as a sheet protector to prevent drying. The camera system allowed to manually adjust the exposure time in order to ensure a perfect picture of the Western Blot.

### 3 Results

#### 3.1 Confirmation of the samples by STR analysis and IHC staining

Short Tandem Repeat analysis:

STR analysis was performed by using the PowerPlex 16® System to confirm, that the SW-982 and U2OS cell lines were used for the following experiments

STR-Locus	your cell line	DSMZ
D3S1358	15	
TH01	9,3	9,3
D21S11	28,30	
D18S51	16,18	
Penta E	13,15	
D5S818	11,13	11,13
D13S317	12,13	12,13
D7S820	9,11	9,11
D16S539	11,12	11,12
CSF1PO	11,12	11,12
Penta D	10,13	
Amelogenin	X	X
vWA	19,20	19,20
D8S1179	14	
TPOX	9,11	9,11
FGA	21,24	

Table 4: STR loci comparison of SW-982 cells

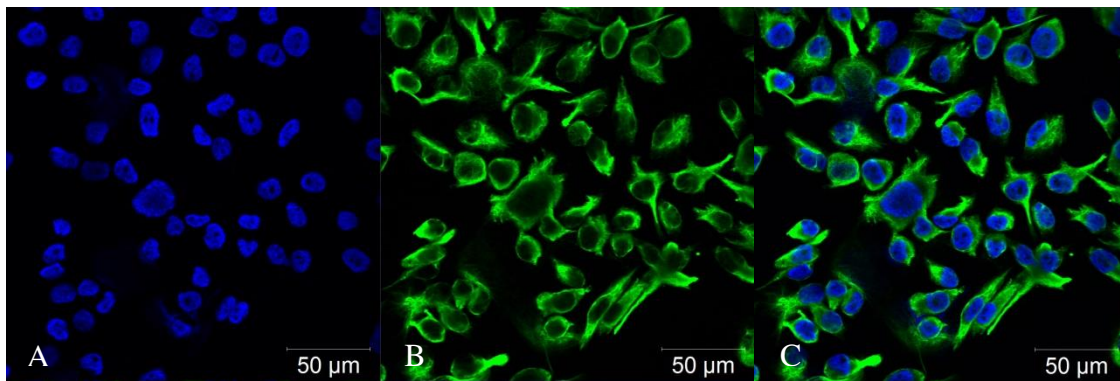
STR-Locus	your cell line	DSMZ
D3S1358	16	
TH01	6, 9.3	6, 9.3
D21S11	31	
D18S51	12,14	
Penta E	10,13	
D5S818	11	11
D13S317	13	13
D7S820	11,12	11,12
D16S539	11,12	11,12
CSF1PO	13	13
Penta D	9	
Amelogenin	X	X
vWA	14,18	14,18
D8S1179	12,14	
TPOX	11,12	11,12
FGA	20	

Table 5: STR loci comparison of U2OS cells

SW-982 and U2OS cell lines matched in the following 9 STR loci as shown in Table 4 and Table 5: TH01, D5S818, D13S317, D7S820, D16S539, CSF1PO, Amelogenin, vWA and TPOX. The results confirmed that the SW-982 and the U2OS cell lines were used for the experiments.

#### Vimentin-DAPI Immunofluorescence analysis:

The vimentin-DAPI immunofluorescence staining was performed to confirm the mesenchymal origin of the SW-982 (Figure 15) and U2OS cell lines (Figure 16). The conformation of the mesenchymal origin of both cell lines was based on the expression of vimentin that was detected by a green fluorescent vimentin-antibody (Figure 15 B and Figure 16 B). Nuclei were stained with 4', 6-diamidino-2-phenylindole (DAPI), which led to a better orientation concerning the imaging and analysis (Figure 15 A and Figure 16 A). Nuclei stained- and vimentin stained pictures were overlaid by using ZEN 2009 software to create the pictures 15 C and 16 C.



**Figure 15: Vimentin-DAPI immunofluorescence staining of the SW-982 cell line**

A: Nuclei were stained with DAPI; B: Vimentin was stained with vimentin-antibody. The expression of vimentin confirmed the mesenchymal origin of the SW-982 cells; C: Nuclei staining (blue) and vimentin staining (green) in an overlay image.

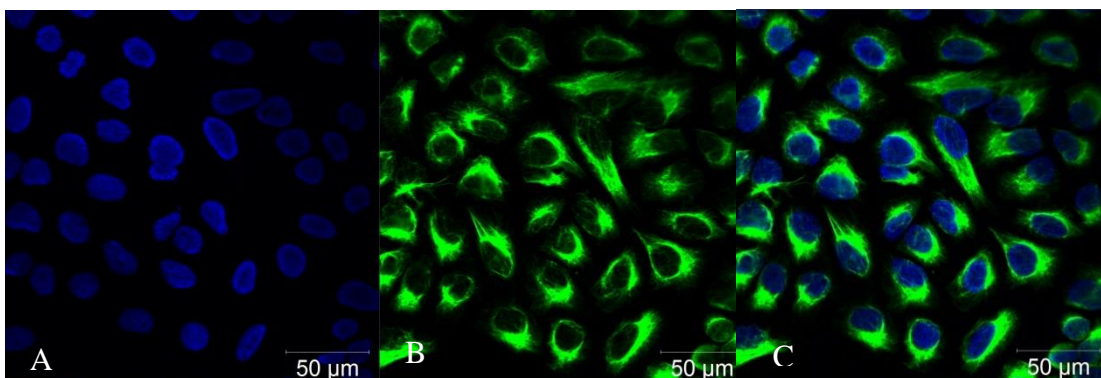


**Figure 16: Vimentin-DAPI immunofluorescence staining of the U2OS cell line**

A: Nuclei were stained with DAPI; B: Vimentin was stained with vimentin-antibody. The expression of vimentin confirmed the mesenchymal origin of the U2OS cells; C: Nuclei staining (blue) and vimentin staining (green) in an overlay image.

### 3.2 Curcumin reduced cell proliferation and viability of sarcoma cell lines SW-982 and U2OS

To investigate the influence of cell viability sarcoma cells (SW-982, SW-1353, U2OS and TE-671) were treated with 0.19  $\mu\text{M}$ , 0.39  $\mu\text{M}$ , 0.78  $\mu\text{M}$ , 1.56  $\mu\text{M}$ , 3.125  $\mu\text{M}$ , 6.25  $\mu\text{M}$ , 12.5  $\mu\text{M}$ , 25  $\mu\text{M}$ , 50  $\mu\text{M}$  and 100  $\mu\text{M}$  Curcumin for 24, 48 and 72 h. The newly produced purple formazan product was measured spectrophotometrically (490 nm) to examine the cell viability. Before performing the measurement, the culture medium that included the different Curcumin dilutions, had to be replaced with fresh culture medium. Figure 17 shows the time- and dose-dependent inhibition of cell viability.

The MTS assay ( $n=4$ ) indicated, that the Curcumin treatment had a significant effect on the cell viability of the SW-982 and U2OS cell lines (Figure 17). Results are mean  $\pm$  standard deviation of three independent experiments measured in quadruplicates.

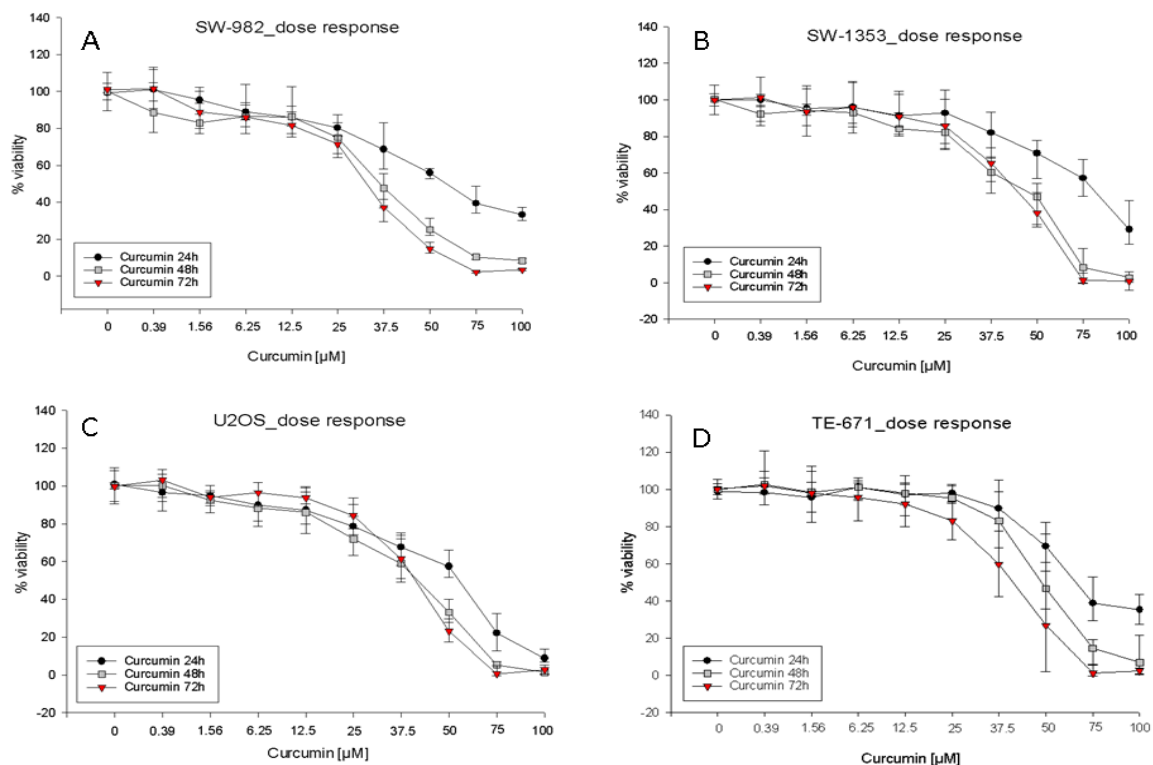


**Figure 17: Influence of DMAS on cell viability of chondrosarcoma cell lines SW-982 (A), SW-1353 (B), U2OS (C) and TE-671 (D).** Cells were treated with 0.19  $\mu\text{M}$ , 0.39  $\mu\text{M}$ , 0.78  $\mu\text{M}$ , 1.56  $\mu\text{M}$ , 3.125  $\mu\text{M}$ , 6.25  $\mu\text{M}$ , 12.5  $\mu\text{M}$ , 25  $\mu\text{M}$ , 50  $\mu\text{M}$  and 100  $\mu\text{M}$  Curcumin for 24, 48 and 72 h. After the incubation over 24, 48 and 72h. The culture medium had to be exchanged before measurement. Curcumin inhibited cell growth in a concentration dependent manner. Untreated cells were measured as controls.

U2OS										
concentration of curcumin	0.00	0.39	1.56	6.25	12.5	25	37.5	50	75	100
24h										
Number of experiments (n)	4	4	4	4	4	4	4	4	4	4
Mean ± SD	100 ± 9.6	94.7 ± 7.7	94.8 ± 5.2	88.9 ± 7.3	86.5 ± 9.2	79.1 ± 4.8	66.5 ± 8.3	58.9 ± 7.1	22.6 ± 9.4	10.2 ± 3.3
p-value	-	0.149	0.120	0.005	0.013	0.000	0.000	0.000	0.000	0.000
48h										
Number of experiments (n)	4	4	4	4	4	4	4	4	4	4
Mean ± SD	100 ± 8.14	100.1 ± 6.19	87.9 ± 8.6	87.9 ± 9.4	90.8 ± 12.8	76.6 ± 13.4	61.6 ± 10.5	33.9 ± 6.2	4.6 ± 2.7	1.9 ± 1.9
p-value	-	0.981	0.002	0.004	0.084	0.000	0.000	0.000	0.000	0.000
72h										
Number of experiments (n)	4	4	4	4	4	4	4	4	4	4
Mean ± SD	100 ± 1.7	105.2 ± 16.9	102.3 ± 17.0	99.2 ± 13.3	99.8 ± 8.9	85.5 ± 9.6	61.4 ± 12.4	23.6 ± 6.1	2.18 ± 2.8	2.8 ± 2.7
p-value	-	0.118	0.442	0.722	0.926	0.000	0.000	0.000	0.000	0.000

Table 6: Mean ± SD and p-values of MTS proliferation assay of all time points of the U2OS cell line.

SW-982										
concentration of curcumin	0.00	0.39	1.56	6.25	12.5	25	37.5	50	75	100
24h										
Number of experiments (n)	4	4	4	4	4	4	4	4	4	4
Mean ± SD	100 ± 4.6	99.8 ± 4.9	93.9 ± 6.3	89.3 ± 4.6	86.7 ± 5.4	81.6 ± 5.9	70.6 ± 12.6	55.5 ± 2.8	41.4 ± 7.3	33.7 ± 3.6
p-value	-	0.149	0.120	0.005	0.013	0.000	0.000	0.000	0.000	0.000
48h										
Number of experiments (n)	4	4	4	4	4	4	4	4	4	4
Mean ± SD	100 ± 10.4	94.8 ± 17.0	85.5 ± 8.3	90.6 ± 13.3	88.9 ± 13.5	73.7 ± 9.5	46.2 ± 9.3	26.7 ± 4.5	10.2 ± 1.1	8.5 ± 1.2
p-value	-	0.981	0.002	0.004	0.084	0.000	0.000	0.000	0.000	0.000
72h										
Number of experiments (n)	4	4	4	4	4	4	4	4	4	4
Mean ± SD	100 ± 4.4	103.5 ± 10.7	91.1 ± 10.5	86.8 ± 5.7	83.1 ± 5.6	71.2 ± 4.5	35.4 ± 5.8	15.3 ± 2.8	2.2 ± 0.6	3.5 ± 0.5
p-value	-	0.118	0.442	0.722	0.926	0.000	0.000	0.000	0.000	0.000

Table 7: Mean ± SD and p-values of MTS proliferation assay of all time points of the SW-982 cell line.

The half maximal inhibitory concentration (IC<sub>50</sub>) of both cell lines for 48 h of treatment is represented in figure 18. The measurement was performed three times without and four times with the exchange of the culture medium.

In case of the SW-982 cells the value for the IC<sub>50</sub> for 48 h of treatment was 29 µM without the exchange of culture medium and 36.2 µM with exchange of the culture medium. The IC<sub>50</sub> value of the U2OS cells for 48 h of treatment was 40.1 µM without the exchange of culture medium and 45.6 µM with exchange of the culture medium.

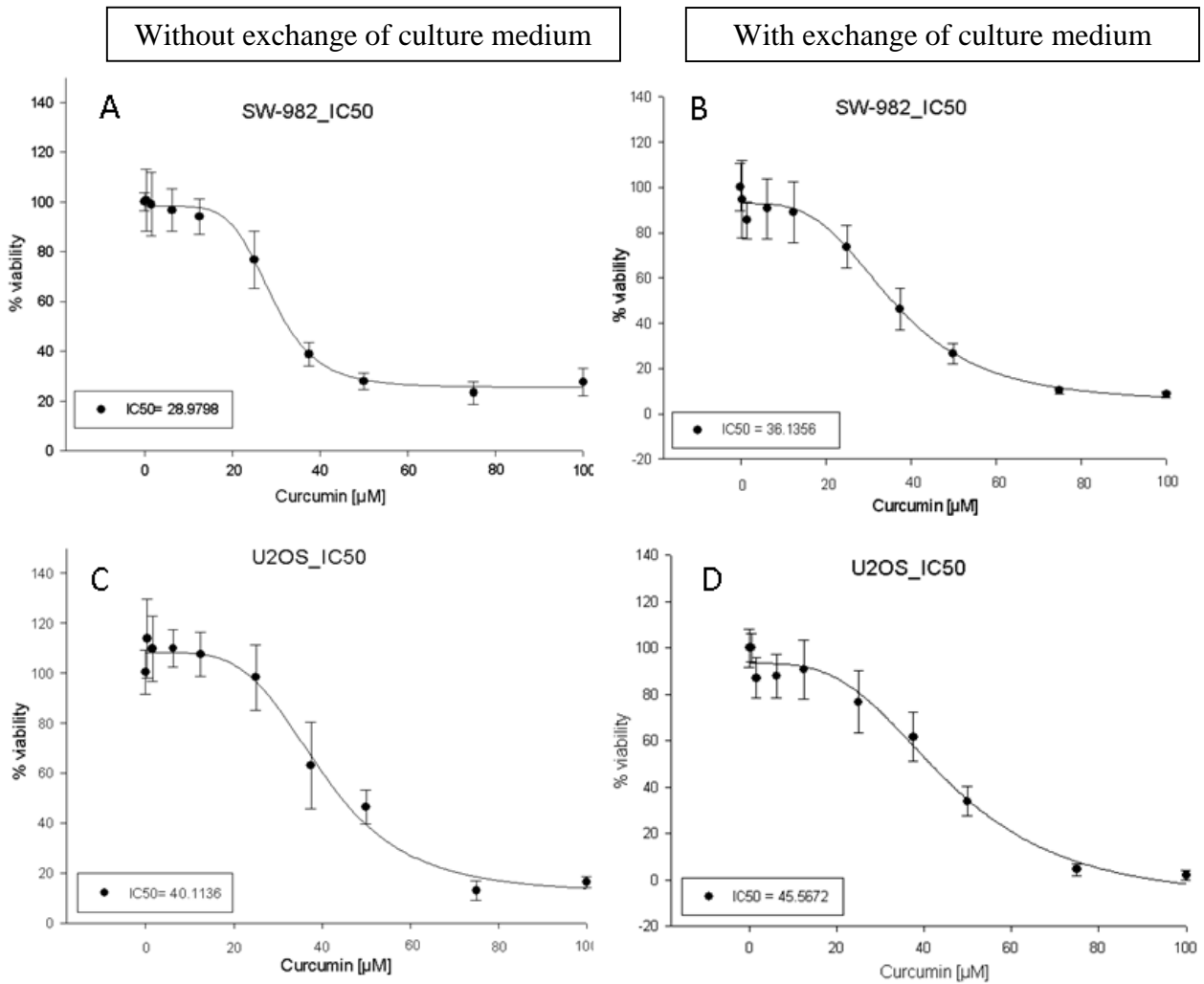


**Figure 18: IC<sub>50</sub>-values of the sarcoma cell lines SW-982 and U2OS for 48 h without (A, C) and with (B, D) exchange of the culture medium before measurement.**

IC<sub>50</sub>-values of both cell lines are included in the figures. For the SW-982 cells the value for the IC<sub>50</sub> for 48 h of treatment was 29 μM (A) without the exchange of culture medium and 36.2 μM (B) with the exchange of the culture medium. The IC-50 value of the U2OS cells for 48 h of treatment was 40.1 μM (C) without the exchange of culture medium and 45.6 μM (D) with the exchange of the culture medium.

The cell lines SW-982 and U2OS were treated with 0.0, 12.5, 25.0 and 50.0  $\mu\text{M}$  curcumin for 72 hours. During this period, cell growth curves were automatically recorded in real time by the xCELLigence System. Curcumin inhibited cell growth in a concentration dependent manner in both cell lines.

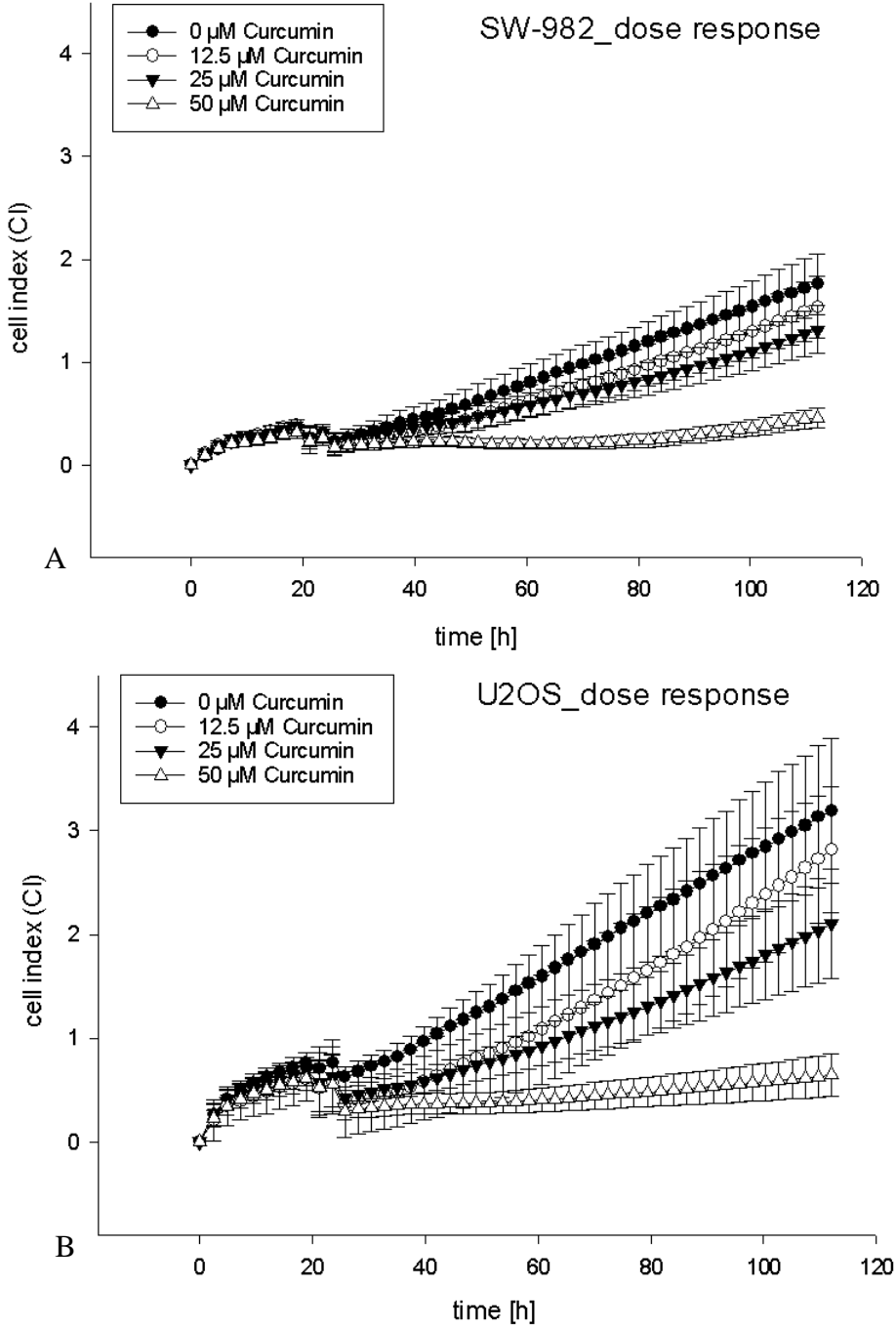


**Figure 19: Influence of curcumin on cell proliferation of sarcoma cell lines SW-982 (A) and U2OS (B).** Dynamic proliferation curves for both cell lines in the presence of 0.0, 12.5, 25.0 and 50.0  $\mu\text{M}$  curcumin.

### 3.3 Curcumin induced apoptosis could not be measured by FACS analysis

Apoptosis can be triggered through different pathways that are based on the proteolytic activity of caspases. Effector caspases such as caspase 3 cleave a large number of cellular proteins like major cytoplasmatic and nuclear elements, which form the biochemical basis of apoptotic cells. To measure the apoptotic status of the SW-982 and U2OS cell lines, curcumin treated cells (0  $\mu\text{M}$ , 18.1  $\mu\text{M}$  and 36.2  $\mu\text{M}$  for the SW-982 cells and 0  $\mu\text{M}$ , 22.8  $\mu\text{M}$  and 45.6  $\mu\text{M}$  for the U2OS cells) were fixed, permeabilized and stained with a cleaved caspase 3 fluorescent antibody, which can be detected by FACS LSR II System. Because of the similar excitation and emission spectra of curcumin and the cleaved caspase 3 fluorescent antibody, a negative control of each sample was used for the normalization that was not stained with the cleaved caspase 3 antibody. 2.7% of the SW-982 cells and 9.5% of the U2OS cells that were treated with the IC<sub>25</sub> concentration of curcumin indicated apoptotic behaviour. 2.7% of the SW-982 cells and 9.5% of the U2OS cells that were treated with the IC<sub>50</sub> concentration of curcumin indicated apoptotic behaviour.

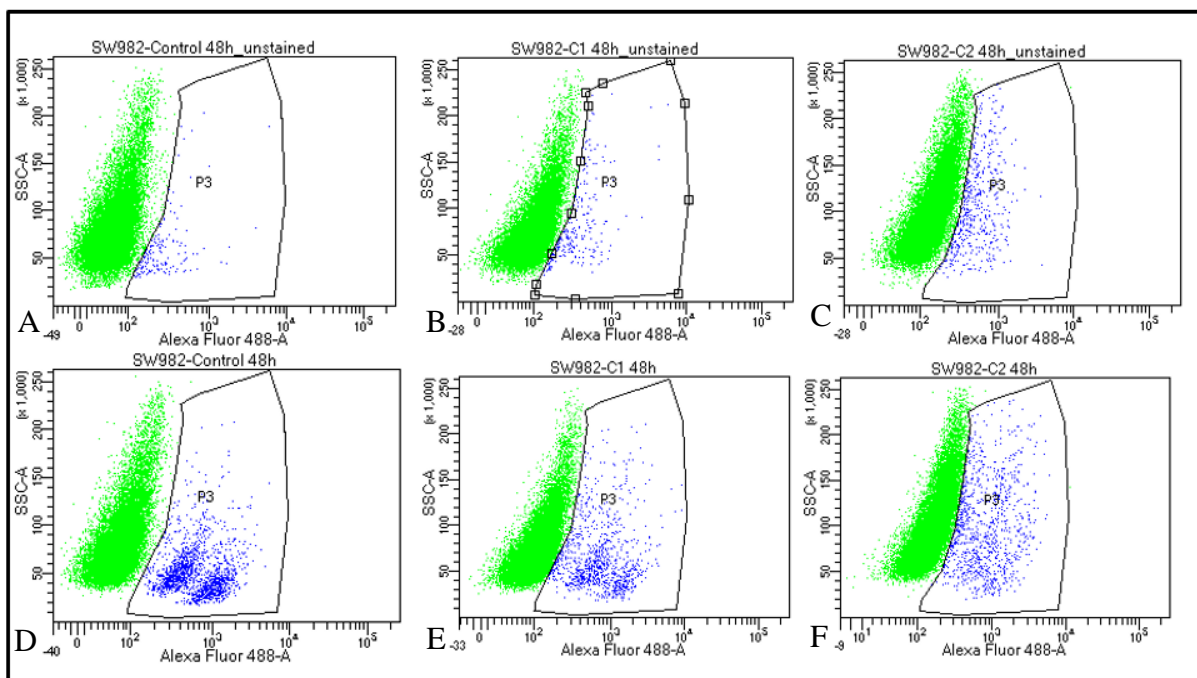


**Figure 20: Results from the cleaved caspase 3 measurement of the SW-982 cells.** Cells were treated with 0  $\mu\text{M}$  (A, D), 18.1  $\mu\text{M}$  (B, E) and 36.2  $\mu\text{M}$  (C, F) curcumin. Because of the similar excitation and emission spectra of curcumin and the cleaved caspase 3 fluorescent antibody, a negative control (A, B and C) of each sample was used for the normalization that was not stained with the cleaved caspase 3 antibody.

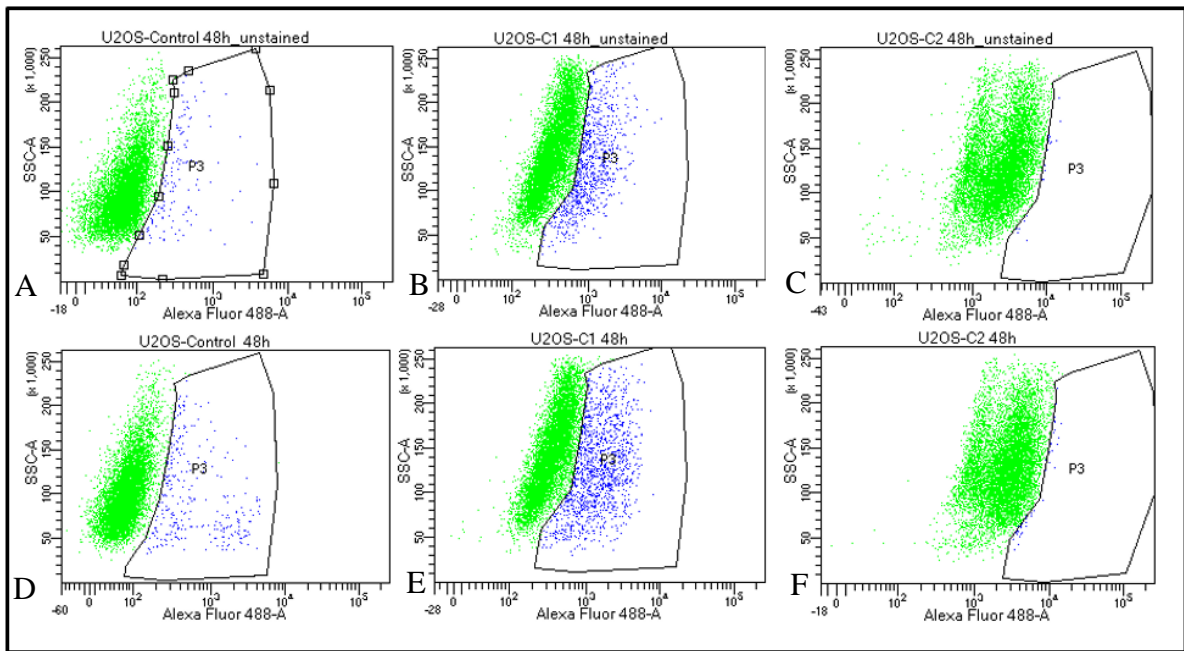


**Figure 21: Results from the cleaved caspase 3 measurement of the U2OS cells.** Cells were treated with 0  $\mu\text{M}$  (A, D), 22.8  $\mu\text{M}$  (B, E) and 45.6  $\mu\text{M}$  (C, F) curcumin. Because of the similar excitation and emission spectra of curcumin and the cleaved caspase 3 fluorescent antibody, a negative control (A, B and C) of each sample was used for the normalization that was not stained with the cleaved caspase 3 antibody.

	IC <sub>25</sub> [apoptotic cells in %]	IC <sub>50</sub> [apoptotic cells in %]
SW-982	2.7	2.7
U2OS	9.5	9.5

**Table 6: Results from the cleaved caspase 3 measurement of the SW-982 and U2OS cells.** Cells were treated with curcumin (0  $\mu\text{M}$ , 18.1  $\mu\text{M}$  and 36.2  $\mu\text{M}$  for the SW-982 cells and 0  $\mu\text{M}$ , 22.8  $\mu\text{M}$  and 45.6  $\mu\text{M}$  for the U2OS cells), stained with a cleaved caspase 3 antibody and samples were measured by using the FACS LSR II System. 2.7% of the SW-982 cells and 9.5% of the U2OS cells that were treated with the IC<sub>25</sub> concentration of curcumin indicated apoptotic behaviour. 2.7% of the SW-982 cells and 9.5% of the U2OS cells that were treated with the IC<sub>50</sub> concentration of curcumin indicated apoptotic behaviour.

To determine another apoptotic marker, the apoptotic effect of curcumin in SW-982 and U2OS cells was evaluated by flow cytometric analysis of Annexin V and propidium iodide (PI) staining. Both cell lines were treated with curcumin (0  $\mu\text{M}$ , 18.1  $\mu\text{M}$  and 36.2  $\mu\text{M}$  for the SW-982 cells and 0  $\mu\text{M}$ , 22.8  $\mu\text{M}$  and 45.6  $\mu\text{M}$  for the U2OS cells). The percentage of early apoptotic cells (Annexin<sup>pos</sup>/PI<sup>neg</sup>) was 0.1%, 0.3% and 0.9% respectively for 6 h for the SW-982 cells and 1.7%, 4.2% and 2.8% for 6 h for the U2OS cells. The percentage of the late apoptotic cells (Annexin<sup>pos</sup>/PI<sup>pos</sup>) was 3.4%, 11.2% and 14.6% for SW-982 cells for 6 h and 2.3%, 6.8% and 9.7% for the U2OS cells.

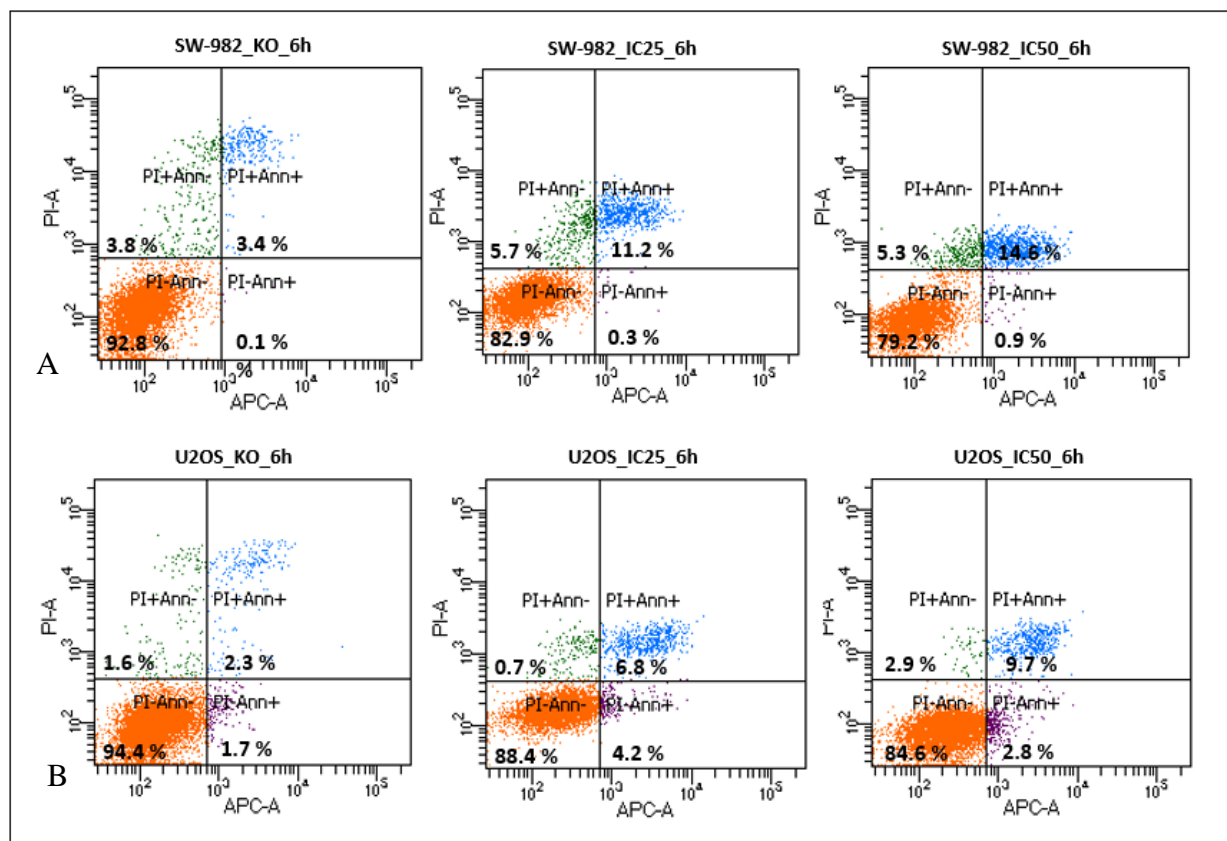


**Figure 22: Curcumin did not induce apoptosis in SW-982 (A) and U2OS (B) cells.** Both cell lines were treated with (0  $\mu\text{M}$ , 18.1  $\mu\text{M}$  and 36.2  $\mu\text{M}$  for the SW-982 cells and 0  $\mu\text{M}$ , 22.8  $\mu\text{M}$  and 45.6  $\mu\text{M}$  for the U2OS cells). The apoptotic status was evaluated by Annexin V-PI binding assay. The lower right part (Annexin<sup>pos</sup>/PI<sup>neg</sup>) was considered as early stage of apoptotic cells and the top right part (Annexin<sup>pos</sup>/PI<sup>pos</sup>) was considered as late stage of apoptotic cells. The lower left part (Annexin<sup>neg</sup>/PI<sup>neg</sup>) was considered as viable cells and the upper left part (Annexin<sup>neg</sup>/PI<sup>pos</sup>) was considered as necrotic cells.

### 3.4 The proteome profiler array identified the highest expressed NFκB proteins

The proteome profiler array (NFκB-assay) was performed to determine the relative levels of selected human NFκB proteins. The array was used as a screening method to choose the highest expressed NFκB proteins, which have been used for further experiments.

Some of these proteins were highly expressed in both cell lines: IKKα, NFκB1, NFκB2, FADD, Fas, IκBa, IκBe, IKK2, RelA and DR4.

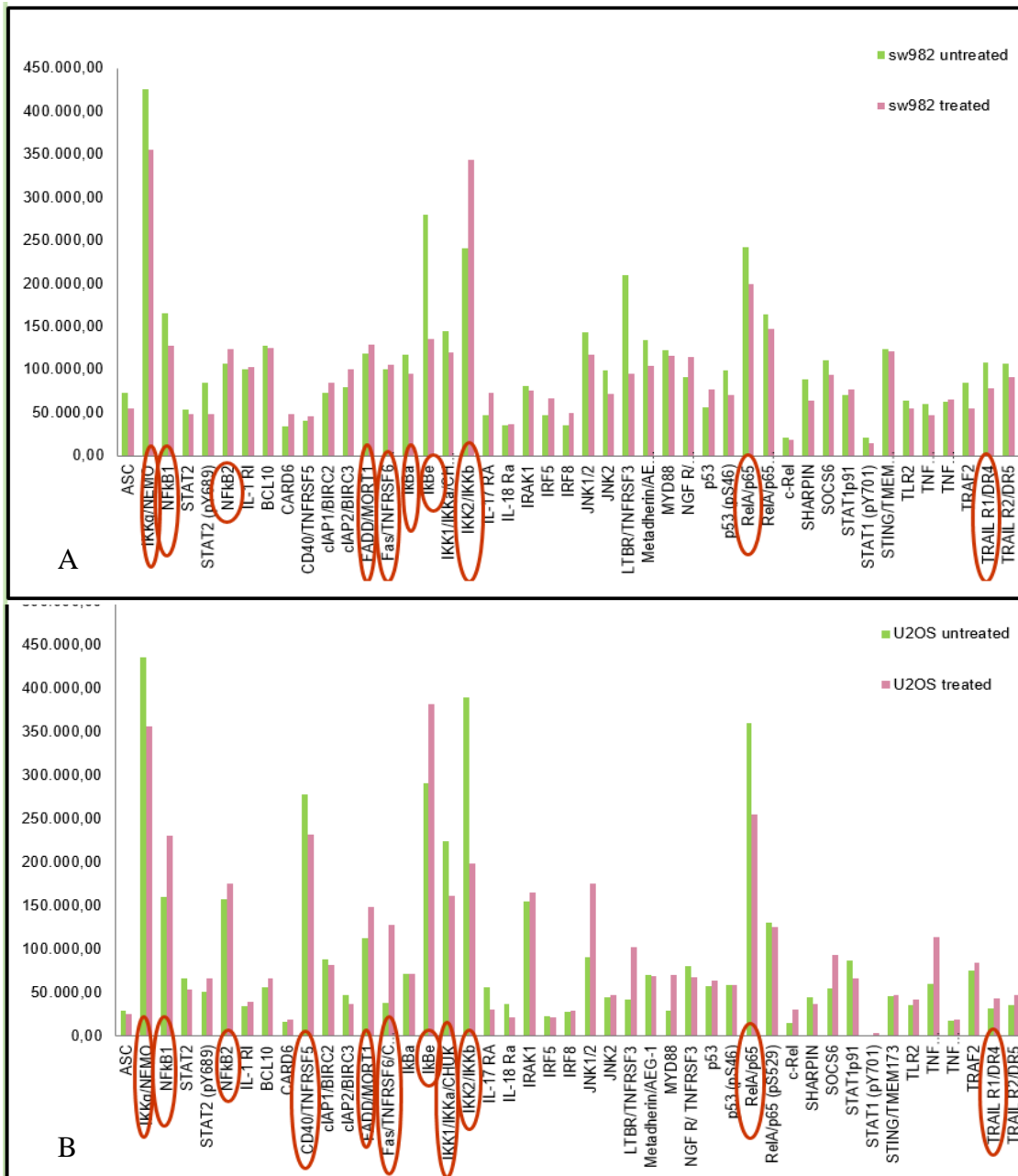


**Figure 23: NFκB assay of untreated and treated SW-982 cells (A) and U2OS cells (B).** Some of these proteins were highly expressed in both cell lines: IKKα, NFκB1, NFκB2, FADD, Fas, IκBa, IκBe, IKK2, RelA and DR4.

### 3.5 Gene expression of FADD, Fas, DR4 and TNFR1 showed an increase in curcumin treated cells

Quantitative Real-time Polymerase Chain Reaction was performed to examine the relative expression of the FAS-associated death domain gene (FADD), the Fas cell surface death receptor gene (FAS), the death receptor 4 gene (DR4) and the tumor necrosis factor receptor 1 gene (TNFR1) with untreated and treated (curcumin) SW-982 and U2OS cells. Relative gene expression was normalized on reference genes (2- $\Delta\Delta C_t$ -method) and data is shown as mean  $\pm$  SD of independent experiments (n=4) performed in triplicates. Gene expression of FADD showed a significant increase in curcumin treated SW-982 (p=0.038) and U2OS cells (p=0.001). The Fas gene expression indicated a significant rise in curcumin treated SW-982 (p=0.015) and U2OS cells (p=0.018) and the DR4 gene expression was significantly increased in curcumin treated SW-982 (p=0.013) and U2OS cells (p=0.010). TNFR1 gene expression showed a non-significant increase in curcumin treated SW-982 cells (p=0.070) and a significant increase in curcumin treated U2OS cells (p=0.029).

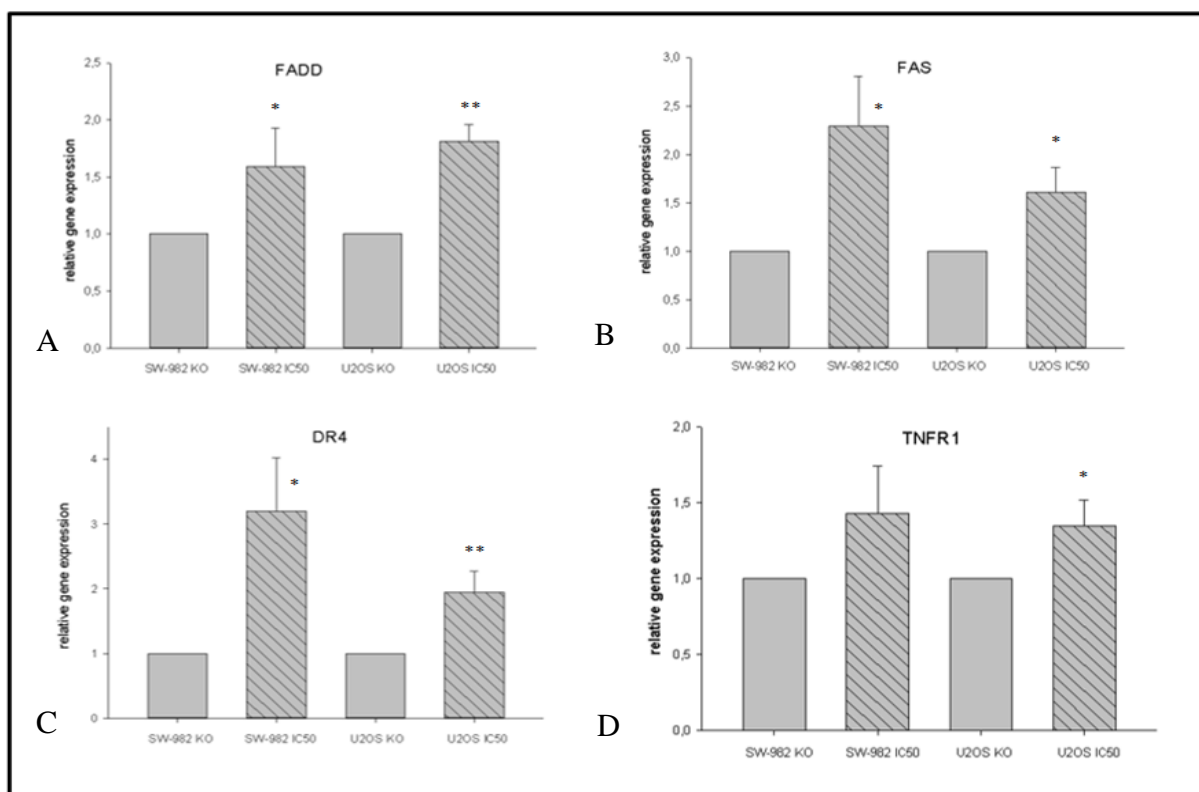


**Figure 24: Relative gene expression levels of FADD, FAS, DR4 and TNFR1 in untreated and treated (curcumin) SW-982 and U2OS cells.** Gene expression of FADD, Fas and DR4 showed a significant increase in curcumin treated SW-982 and U2OS cells (A, B, C). TNFR1 gene expression indicated a non-significant increase in curcumin treated SW-982 cells and a significant increase in curcumin treated U2OS cells (D).

### 3.6 Curcumin induced cell damage but didn't induce apoptosis

Western Blots were performed to examine the gene expression of H2AX, PARP and cleaved PARP with untreated and treated (curcumin) SW-982 and U2OS cells. H2AX is an indicator for cell damage and cleaved PARP indicates apoptosis.

Data is shown as mean  $\pm$  SD of independent experiments (n=2) performed.

Gene expression of H2AX showed a non-significant increase in curcumin treated SW-982 and U2OS cells. The cleaved PARP gene expression didn't indicate a rise in curcumin treated SW-982 and only a low non-significant increase in curcumin treated U2OS cells.

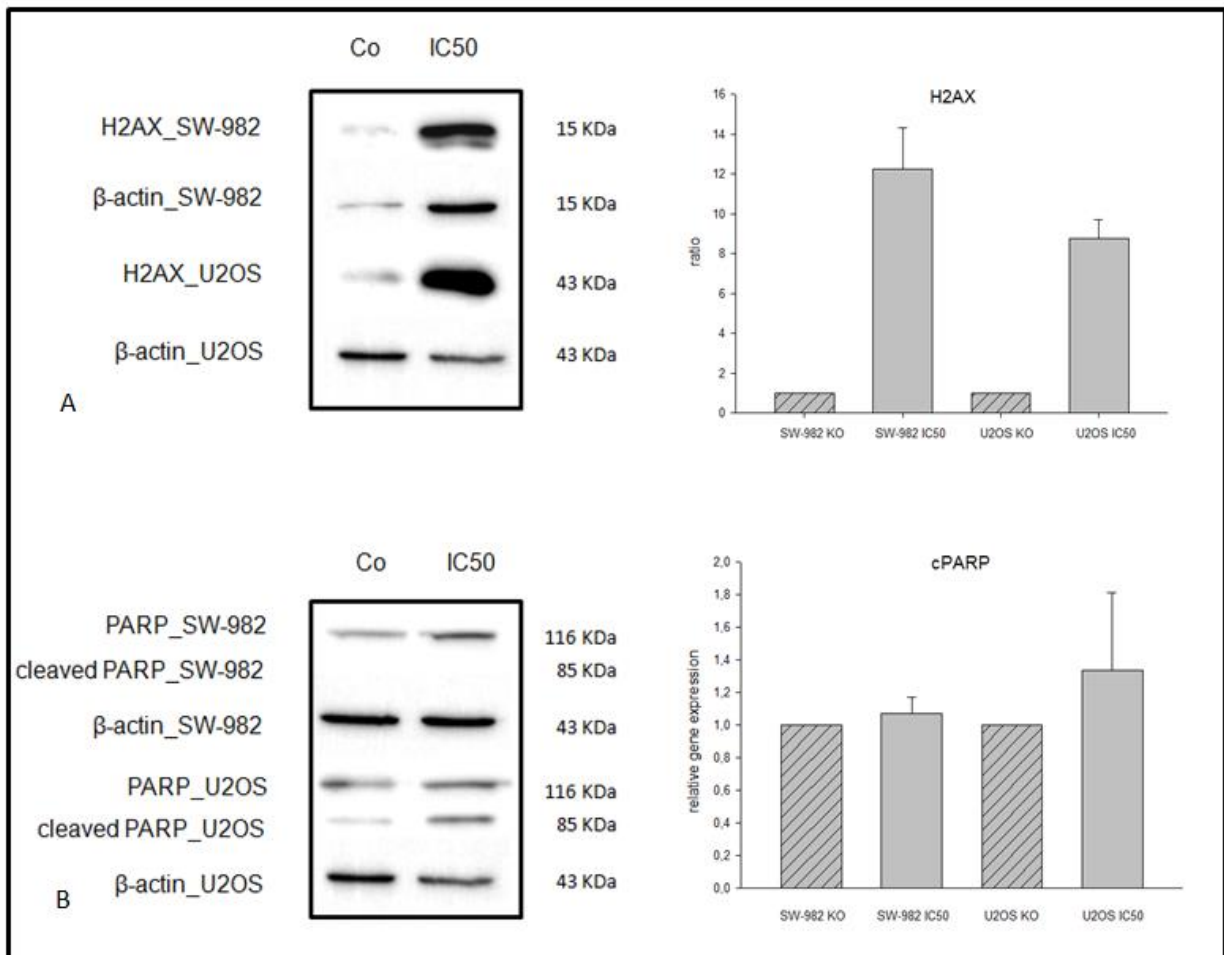


**Figure 25: Gene expression of H2AX (A), PARP and cleaved PARP (B) in untreated and treated (curcumin) SW-982 and U2OS cells.** The molecular weight of H2AX is 15 KDa and is used as an indicator for cell damage. Gene expression of H2AX showed a non-significant increase in curcumin treated SW-982 and U2OS cells. The molecular weight of PARP is 116 KDa and the size of cleaved PARP is 85 KDa, which is used as an indicator for apoptosis. The cleaved PARP gene expression didn't indicate a rise in curcumin treated SW-982 and only a low non-significant increase in curcumin treated U2OS cells.

### 3.7 Curcumin influenced NFκB-pathway

Western Blots were performed to examine the gene expression of unphosphorylated and phosphorylated IκBα, p65 and p50 in untreated and treated (curcumin) SW-982 and U2OS cells. IκB-α belongs to the IκB family which inhibit binding of p50-p65 NFκB complex or Rel protein to their cognate binding sites but do not inhibit the binding of p50 homodimer to NFκB sites.

Data is shown as mean ± SD of independent experiments (n=2) performed in duplicates.

Gene expression of the phosphorylated IκB-α showed a non-significant decrease in curcumin treated SW-982 and U2OS cells. The phosphorylated p65 gene expression indicated a non-significant decrease in curcumin treated SW-982 and U2OS cells and the gene expression of the phosphorylated p50 showed a non-significant increase in curcumin treated SW-982 and U2OS cells.

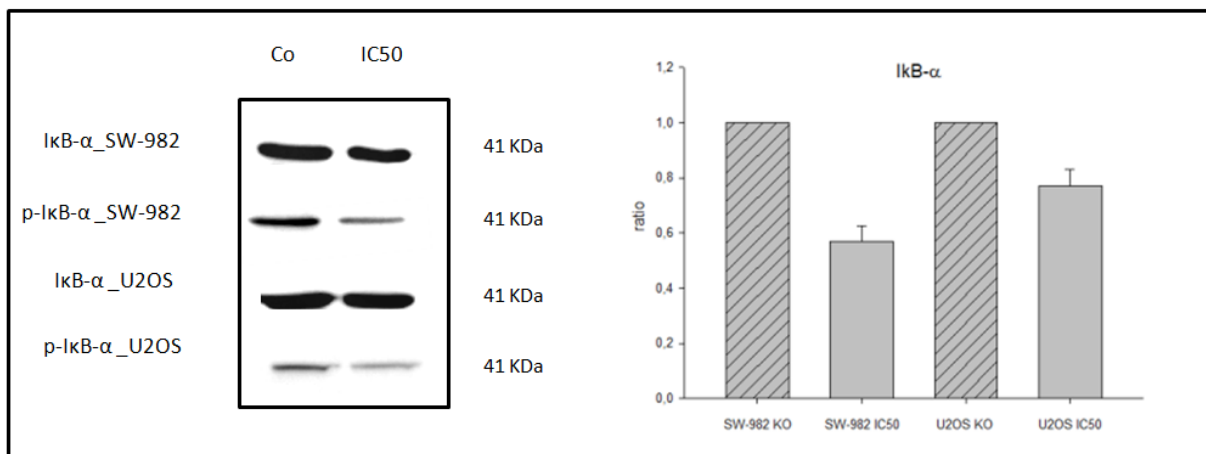


**Figure 26: Gene expression of unphosphorylated and phosphorylated IκB-α in untreated and treated (curcumin) SW-982 and U2OS cells.** The molecular weight of the unphosphorylated and phosphorylated IκB-α is 41 KDa. Gene expression of the phosphorylated IκB-α showed a significant decrease in curcumin treated SW-982 (p=xxx) and U2OS cells (p=xxx).

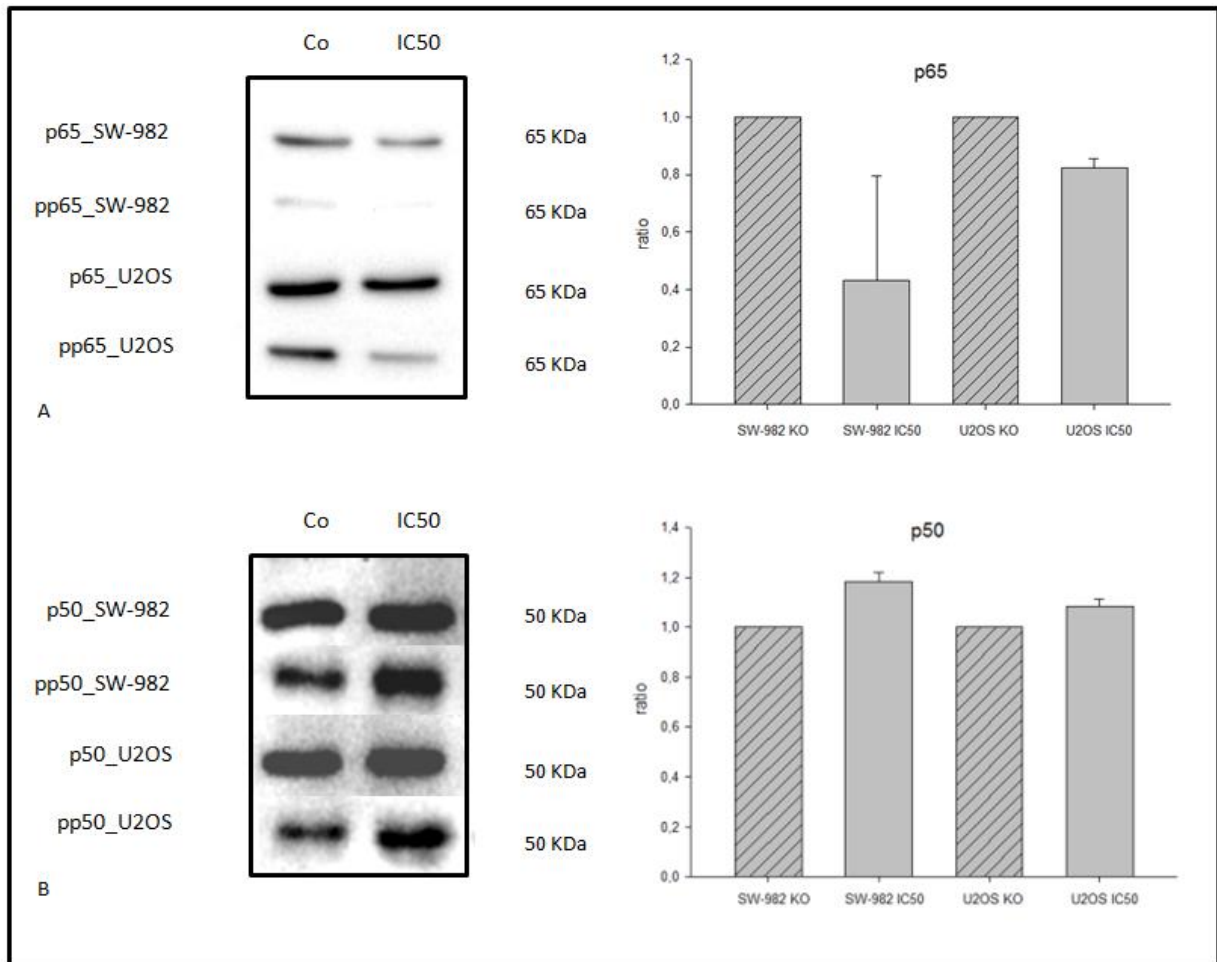


**Figure 27: Gene expression of unphosphorylated and phosphorylated p65 and p50 in untreated and treated (curcumin) SW-982 and U2OS cells.** The molecular weight of the unphosphorylated and phosphorylated p65 is 65 KDa and the size of the unphosphorylated and phosphorylated p50 is 50 KDa. Gene expression of the phosphorylated p65 showed a non-significant decrease in curcumin treated SW-982 and U2OS cells and the gene expression of the phosphorylated p50 showed a significant increase in curcumin treated SW-982 and U2OS cells.

## 4 Discussion

Synovial sarcoma (SS) is a high-grade, malignant STS accounting for 5–10% of STS. [14-16] After rhabdomyosarcoma, SS is the most common STS in children, adolescents, and young adults. [18] Metastases occur in 50–70% of cases. Since these tumors grow slowly, they have a high incidence of late metastases [27], as reflected in the difference between 5-year and 10-year survival. Osteosarcoma (OS) is a deadly form of musculoskeletal cancer that most commonly causes patients to die of pulmonary metastatic disease. [34, 35] The overall 5-year survival rate for patients diagnosed between 1974 and 1994 was 63%.

The development of new therapeutic agents targeting the malignant behaviour of synovial- and osteosarcoma cells is important to improve the prognosis. [98] Curcumin a yellow pigment and spice in turmeric and curry, exhibits anticarcinogenic effects. [99] The therapeutic values of curcumin have been proven in human clinical studies [100]. More important, curcumin is safe in humans even at a dose of 10 g/day [101]. However the anti-cancer-effects of curcumin on SS and OS cells are mostly unknown.

In 2015 Dazhi Yu et al. demonstrated that curcumin significantly inhibited the proliferation of MG-63 (OS) cells. With our study it could be shown that the same effect could be observed in the two sarcoma cell lines SW-982 (SS) and U2OS (OS). Curcumin decreased the cell viability and the cell proliferation in a dose dependent manner. [102]

Performing the MTS – assay for the examination of the  $IC_{50}$  values led to some problems because of the similar excitation- and emission spectra of curcumin and the used MTS-reagent. The yellow colour of curcumin was influencing the spectrometric measurement, which led to lower  $IC_{50}$  values, without the exchange of the culture medium. To solve this problem, the culture medium was exchanged, before the spectrometric measurement of the samples. In case of the SW-982 cells the value for the  $IC_{50}$  for 48 h of treatment was 29  $\mu$ M without the exchange of culture medium and 36.2  $\mu$ M with exchange of the culture medium. The  $IC_{50}$  value of the U2OS cells for 48 h of treatment was 40.1  $\mu$ M without the exchange of culture medium and 45.6  $\mu$ M with exchange of the culture medium.

In 2014 Run Chang illustrated for the first time that curcumin induced greater cytotoxicity on MG-63 OS cells than on healthy human osteoblasts in a dose-dependent manner.

Although in this study no  $IC_{50}$  value was examined, the results from this study suggest that curcumin at a concentration of 25  $\mu\text{M}$  decreased OS over healthy osteoblast density the most. [103] In 2014 Santosh S. Dhule et al. examined the effect of liposomal curcumin on the two OS cell lines KHOS, MG-6. Additionally, based on earlier results, liposomal curcumin is known to be 4–5 times more effective than curcumin as a pure compound against OS. In case of the KHOS cells the value for the  $IC_{50}$  for 48 h of treatment was  $6.36 \pm 2.6 \mu\text{M}$  and the  $IC_{50}$  value of the MG-6 cells for 48 h of treatment was  $8.62 \pm 0.3 \mu\text{M}$ . [104] These two studies show similar ranges of  $IC_{50}$  values, which confirm our received results.

The apoptotic behaviour of both cell lines was examined by FACS analysis and was confirmed by Western Blot analysis of the gene expression of cleaved PARP, which was used as an apoptosis indicator. But in contrast to the results of Zhongping Fu et al. [105], who observed apoptotic behaviour in VEGF tumor cells and Hsiang-Ping Lee et al. [106], who determined apoptosis in chondrosarcoma cell, no apoptotic effect could be observed in the SW-982 cells and only a very low one in the U2OS cells, concerning 9.5% of all U2OS cells. Because of the similar excitation and emission spectra of curcumin and the fluorescent antibodies, a negative control of each sample was used for the normalization of the samples that was not stained with the antibody. Without this normalization step the measurement could be misinterpreted which could lead to wrong positive apoptotic results.

In 2011 Dennis Ma et al. evaluated the combinatorial effects of curcumin and a drug called JCTH-4 in OS cells. Curcumin alone at 5  $\mu\text{M}$  had no significant effect on Saos-2 and U2OS cells. However, when used in combination, Curcumin was able to selectively potentiate the effect of JCTH-4 in these OS cell lines. Although apoptotic effects could be observed without the treatment of curcumin, a much higher apoptotic effect was achieved by adding curcumin, thus leading to the conclusion that curcumin potentiates the used drug. [107]

In 2013 W. Shannon Orr et al. observed that curcumin potentiates rhabdomyosarcoma radiosensitivity by suppressing NF- $\kappa$ B activity. Cells were next treated with 10  $\mu\text{M}$  liposomal curcumin prior to radiation exposure and then analysed by FACS for apoptosis by Annexin V-staining 48 h after irradiation. The combination of curcumin and radiation significantly increased apoptosis compared to control in both cell lines. Apoptosis in control Rh30 cells was  $4.6\% \pm 0.41$  as compared to  $8.67\% \pm 0.64$  or  $7.5\% \pm 0.3$  in cells treated with radiation, or curcumin

alone, respectively. In contrast apoptosis in Rh30 cells treated with a combination of radiation and curcumin was  $19.5\% \pm 0.54$  ( $p = .00003$ ). [108]

Western Blot analysis was also performed to measure the cell damage in untreated and treated SW-982 and U2OS cells. The expression of H2AX, an indicator for cell damage, in both cell lines was examined, which led to the conclusion that curcumin induces cell damage in both cell lines.

DNA damage induction and repair after treatment with curcumin was examined by Ekram M. Saleh et al. in 2012. H2AX foci are formed upon DNA damage and were often taken as a marker of DNA DSBs. In the study they found that doses as low as  $10\mu\text{g/ml}$  curcumin could induce H2AX foci in MCF7, HepG2, HCT116 and HeLa cells. The fraction of DNA released, as determined by CFGE for all tumor cell lines was found to increase with treatment dose. [109]

In addition a proteome profiler array (NF $\kappa$ B-assay) was performed to determine the relative levels of selected human NF $\kappa$ B proteins. The array was used as a screening method to choose the highest expressed NF $\kappa$ B proteins, which have been used for further experiments.

With four of these highly expressed genes (FADD, FAS, DR4 and TNFR1) a quantitative Real-time Polymerase Chain Reaction was performed to examine the relative expression of the genes in untreated and treated (curcumin) SW-982 and U2OS cells. Gene expression of FADD, Fas and DR4 showed a significant increase in curcumin treated SW-982 and U2OS cells. TNFR1 gene expression indicated a non-significant increase in curcumin treated SW-982 cells and a significant increase in curcumin treated U2OS cells.

In 2001 Bush, J.A could observe the upregulation of cell membrane receptors in human melanoma cells (Fas, TRAIL) [110] and Moragoda, L. et al noted a curcumin induced increase of FADD and Fas in gastric and colon cancer cells. [111]

Curcumin influenced the gene expression of I $\kappa$ B- $\alpha$ , p65 and p50 which play an important role in the NF $\kappa$ B pathway. P65 and p50 belong to the NF $\kappa$ B family, which are transcription factors that form hetero- and homodimers that remain inactive in the cytoplasm when associated with I $\kappa$ B proteins. I $\kappa$ B- $\alpha$  belongs to the I $\kappa$ B family which inhibit binding of p50-p65 NF $\kappa$ B complex or Rel protein to their cognate binding sites but do not inhibit the binding of p50 homodimer to NF $\kappa$ B sites, suggesting that the I $\kappa$ B- $\alpha$  family binds to the p65 subunit of p50-p65 hetero complex through ankyrin repeats. [112] Activation of I $\kappa$ B kinases like I $\kappa$ B- $\alpha$  results in the phosphorylation of the inhibitory I $\kappa$ B- $\alpha$  protein bound to NF $\kappa$ B. NF $\kappa$ B is then released and translocates to the nucleus where it interacts with other transcription factors and transcriptional co-factors to regulate expression of an array of genes. [113]

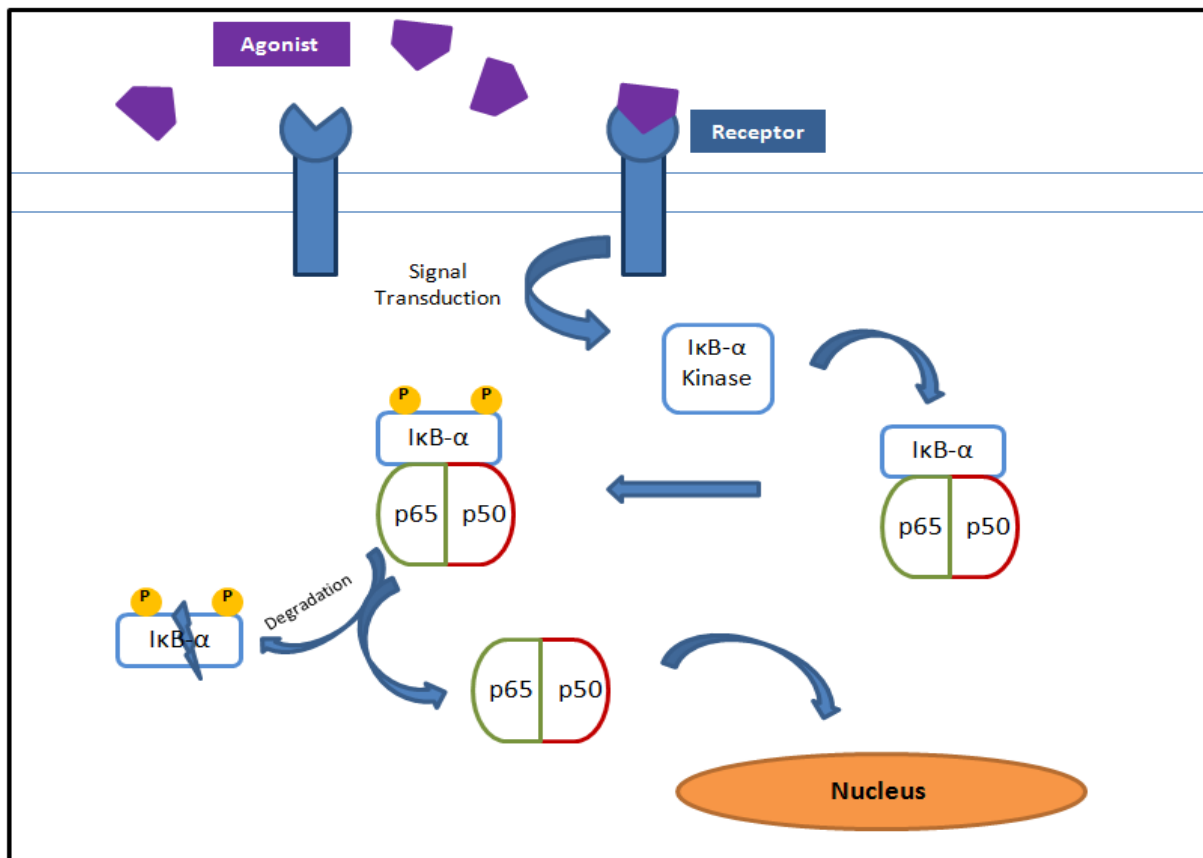


**Figure 28: Inactive (unphosphorylated) I $\kappa$ B- $\alpha$  inhibits NF $\kappa$ B heterodimer p65/p50**

The NF $\kappa$ B proteins p65 and p50 form a heterodimer and are inhibited by the cytoplasmic inhibitory protein I $\kappa$ B- $\alpha$ . After activation of external stimuli the heterodimer can become activated by the activation of I $\kappa$ B- $\alpha$  kinase, which leads to the phosphorylation of I $\kappa$ B- $\alpha$ , followed by the proteasomal degradation of this factor. Thus the NF $\kappa$ B heterodimer p65/p50 gets released and translocates to the nucleus, where it can activate the transcription of its target genes.

Many different types of human tumors have misregulated NF- $\kappa$ B, that NF- $\kappa$ B is constitutively active. The active form of NF $\kappa$ B up-regulates the expression of genes that keep the cell proliferating and protect the cell from conditions that would cause the cells to die. [114]

In tumor cells, NF- $\kappa$ B is active either due to mutations in genes encoding the NF- $\kappa$ B transcription factors themselves or in genes that control NF- $\kappa$ B activity such as I $\kappa$ B genes. Or some tumor cells secrete factors that cause NF- $\kappa$ B to become active. Blocking NF- $\kappa$ B can cause tumor cells to stop proliferating, to die or to become more sensitive to the action of anti-tumor agents. [115]

Treatment of the sarcoma cell lines with curcumin, a naturally occurring inhibitor of NF- $\kappa$ B activity, showed a decrease in the gene expression of the phosphorylated I $\kappa$ B- $\alpha$  and thus, like Dazhi Yu et al. examined [116], led to a inhibition of the binding of p65-complexes to their cognate binding sites.

In contrast to p65 the binding of p50 to NF $\kappa$ B sites was not inhibited, suggesting that the I $\kappa$ B- $\alpha$  family binds to the p65 subunit of p50-p65 hetero complex.

In 2011 Reason Wilken et al. had shown that curcumin has an inhibitory effect on NF $\kappa$ B activation mediated through inhibition of I $\kappa$ B and results in inactive NF- $\kappa$ B remaining bound to I $\kappa$ B- $\alpha$  in the cytoplasm. As a result curcumin suppresses the activation of NF $\kappa$ B via inhibition of I $\kappa$ B- $\alpha$  activity, leading to suppression of many NF $\kappa$ B -regulated genes involved in tumorigenesis. [117]

In 2010 Marie-Hélène Teiten summed up some results of the inhibitory effect of curcumin on cancer cells, where it was shown that it suppresses the activation of I $\kappa$ B $\alpha$  kinase (IKK), the phosphorylation and degradation of I $\kappa$ B $\alpha$  and the subsequent phosphorylation and nuclear translocation of the p65 subunit in several cancer and premalignant cell types [112–124]. This prevention of NF- $\kappa$ B activation is also related to the ability of curcumin to inhibit the proteasome function [125-127]

Because of its influencing effect on the progression and initiation of cancer, the NF- $\kappa$ B signaling pathway is known to be an important node of pharmacological research for the development of new drugs. Since NF- $\kappa$ B is also an essential player in the immune response against cancer, there have always been different opinions to use NF- $\kappa$ B inhibitors in the treatment of malignancies. Nevertheless, combining classical chemotherapeutics with inhibitors of NF- $\kappa$ B activation seems to result in promising synergies. Most cancer drugs are cytotoxic agents, which drive proliferating cells into apoptosis. Increased NF- $\kappa$ B activity grants the cancer cells a survival mechanism by the up-regulation of anti-apoptotic genes, which represents a major factor for drug resistance [128-131]. Inhibition of NF- $\kappa$ B is also thought to be at least one mechanism of action of proteasome inhibitors in cancer treatment as activation of NF- $\kappa$ B requires the proteasomal degradation of I $\kappa$ B molecules. [132-134]

## 5 References

1. <https://www.ncbi.nlm.nih.gov/books/NBK9963/> (The Cell: A Molecular Approach. 2nd edition, The Development and Causes of Cancer
2. Jemal A, Tiwari RC, Murray T, et al. Cancer statistics, 2004. *CA Cancer J Clin* 2004; 54: 8–29.
3. DeVita VT Jr, Hellman S, Rosenberg SA, eds. *Cancer: Principles and Practice of Oncology*. 6th ed. Philadelphia, PA: Lippincott Williams & Wilkins, 2001: 1841–1891.
4. Coindre JM, Terrier P, Guillou L, et al. Predictive value of grade for metastasis development in the main histologic types of adult soft tissue sarcomas: a study of 1240 patients from the French Federation of Cancer Centers Sarcoma Group. *Cancer* 2001; 91: 1914–1926.
5. Ismaila A. Adigun, FWACS, FICS; Ganiyu A. Rahman, FWACS, FICS; Mikhaila O. Buhari, FWACP; Kolawole O. Ogundipe, MBBS; and John A. Omotayo, Soft-Tissue Sarcoma in Black Africans: Pattern, Distribution and Management Dilemma, *Journal of the national medical association*, 2007, 99:2: 88-93
6. Brady MS, Gaynor JJ, Brennan MF. Radiation-associated sarcoma of bone and soft tissue. *Arch Surg* 1992; 127: 1379.
7. Zahm SH, Fraumeni JF Jr. The epidemiology of soft tissue sarcoma. *Semin Oncol* 1997; 24: 504–514.
8. Hardell L, Sandström A. A case-control study: soft tissue sarcoma and exposure to phenoxyacetic acids or chlorophenols. *Br J Cancer* 1979; 39: 711–717.
9. Smith AH, Pearce NE, Fisher DO. Soft tissue sarcoma and exposure to phenoxyherbicides and chlorophenols in New Zealand. *J Nat Cancer Inst* 1984; 73: 1111.
10. Levine EA. Prognostic factors in soft tissue sarcoma. *Semin Surg Oncol* 1999; 17.
11. Vorburger SA, Hunt KK. Experimental Approaches, in Pollock RE (ed). *Soft Tissue Sarcomas*. Hamilton, Ontario, BC Decker, Inc., 2002: 89–109.
12. Latres E, Drobnjak M, Pollack D, et al. Chromosome 17 abnormalities and TP53 mutations in adult soft tissue sarcomas. *Am J Pathol* 1994; 145: 345–355.
13. Hieken TJ, Das Gupta TK. Mutant p53 expression: a marker of diminished survival in well-differentiated soft tissue sarcoma. *Clin Cancer Res* 1996; 2: 1391–1395.
14. Bernd Kasper, Thierry Gil, Veronique D'Hondt, Michael Gebhart, Ahmad Awada, Novel treatment strategies for soft tissue sarcoma, *Critical Reviews in Oncology/Hematology* 62, 2007: 9–15
15. Weiss S, Goldblum J, Publishing M., Enzinger and Weiss's *Soft Tissue Tumors*, 2001 St Louis, MIMosby
16. Milchgrub S, Ghandur-Mnaymneh L, Dorfman HD, Albores-Saavedra J. Synovial sarcoma with extensive osteoid and bone formation, *Am J Surg Pathol*, 1993, vol. 17 (pg. 357-363)
17. Miettinen M, Virtanen I. Synovial sarcoma—a misnomer, *Am J Pathol*, 1984, vol. 117 (pg. 18-25)

18. Smith ME, Fisher C, Wilkinson LS, Edwards JC. Synovial sarcoma lack synovial differentiation, *Histopathology* , 1995, vol. 26 (pg. 279-281)
19. Haldar M, Hancock JD, Coffin CM, et al. . A conditional mouse model of synovial sarcoma: insights into a myogenic origin, *Cancer Cell* , 2007, vol. 11 (pg. 375-388)
20. Lewis JJ, Antonescu CR, Leung DH, et al. . Synovial sarcoma: a multivariate analysis of prognostic factors in 112 patients with primary localized tumors of the extremity, *J Clin Oncol* , 2000, vol. 18 (pg. 2087-2094)
21. Okcu MF, Munsell M, Treuner J, et al. . Synovial sarcoma of childhood and adolescence: a multicenter, multivariate analysis of outcome, *J Clin Oncol* , 2003, vol. 21 (pg. 1602-1611)
22. Fletcher CDM, Unni KK, Mertens F. , World Health Organization Classification of Tumours: Pathology and Genetics of Tumours of Soft Tissue and Bone , 2002Lyon, FranceIARC Press
23. Ferrari A, Gronchi A, Casanova M, et al. . Synovial sarcoma: a retrospective analysis of 271 patients of all ages treated at a single institution, *Cancer* , 2004, vol. 101 (pg. 627-634)
24. Ladanyi M, Antonescu CR, Leung DH, et al. . Impact of SYT-SSX fusion type on the clinical behavior of synovial sarcoma: a multi-institutional retrospective study of 243 patients, *Cancer Res* , 2002, vol. 62 (pg. 135-140)
25. Guillou L, Benhattar J, Bonichon F, et al. . Histologic grade, but not SYT-SSX fusion type, is an important prognostic factor in patients with synovial sarcoma: a multicenter, retrospective analysis, *J Clin Oncol* , 2004, vol. 22 (pg. 4040-4050)
26. Kawai A, Woodruff J, Healey JH, et al. . SYT-SSX gene fusion as a determinant of morphology and prognosis in synovial sarcoma, *N Engl J Med* , 1998, vol. 338 (pg. 153-160)
27. Nilsson G, Skytting B, Xie Y, et al. . The SYT-SSX1 variant of synovial sarcoma is associated with a high rate of tumor cell proliferation and poor clinical outcome, *Cancer Res* , 1999, vol. 59 (pg. 3180-3184)
28. Singer S, Baldini EH, Demetri GD, et al. . Synovial sarcoma: prognostic significance of tumor size, margin of resection, and mitotic activity for survival, *J Clin Oncol* , 1996, vol. 14 (pg. 1201-1208)
29. Pisters PW, O'Sullivan B, Maki RG. Evidence-based recommendations for local therapy for soft tissue sarcomas, *J Clin Oncol* , 2007, vol. 25 (pg. 1003-1008)
30. Sakabe T, Murata H, Konishi E, et al. . Evaluation of clinical outcomes and prognostic factors for synovial sarcoma arising from the extremities, *Med Sci Monit* , 2008, vol. 14 (pg. CR305-C310)
31. Goodlad JR, Fletcher CD, Smith MA. Surgical resection of primary soft-tissue sarcoma. Incidence of residual tumour in 95 patients needing re-excision after local resection, *J Bone Joint Surg Br* , 1996, vol. 78 (pg. 658-661)
32. Maduekwe UN, Hornicek FJ, Springfield DS, et al. . Role of sentinel lymph node biopsy in the staging of synovial, epithelioid, and clear cell sarcomas, *Ann Surg Oncol* , 2009, vol. 16 (pg. 1356-1363)
33. A. H. Krieg F. Hefti B. M. Speth G. Jundt L. Guillou U. G. Exner A. R. von Hochstetter M. D. Cserhati B. Fuchs E. Mouhsine, Synovial sarcomas usually metastasize after >5 years: a multicenter retrospective analysis with minimum follow-up of 10 years for survivors, *Annals of Oncology*, 2011; 22:2: 458-467

34. Marulanda GA, Henderson ER, Johnson DA, Letson GD, Cheong D. Orthopedic surgery options for the treatment of primary osteosarcoma. *Cancer Control*. 2008 Jan. 15(1):13-20.
35. Vander Griend RA. Osteosarcoma and its variants. *Orthop Clin North Am*. 1996 Jul. 27(3):575-81.
36. Peltier LF. Tumors of bone and soft tissues. *Orthopedics: A History and Iconography*. San Francisco, Calif: Norman Publishing; 1993. 264-91.
37. Campanacci M. Preface. *Bone and Soft Tissue Tumors: Clinical Features, Imaging, Pathology and Treatment*. 2nd ed. New York, NY: Springer-Verlag; 1999.
38. Weis LD. Common malignant bone tumors: osteosarcoma. Simon MA, Springfield D, eds. *Surgery for Bone and Soft-Tissue Tumors*. Philadelphia, Pa: Lippincott-Raven; 1998. 265-74.
39. Link MP, Eilber F. Osteosarcoma. Pizzo PA, Poplack DG, eds. *Principles and Practice of Pediatric Oncology*. 3rd ed. Philadelphia, Pa: Lippincott-Raven; 1997. 889-920.
40. Arceci RJ, Weinstein HJ. Neoplasia. Avery GB, Fletcher MA, MacDonald MG, eds. *Neonatology: Pathophysiology and Management of the Newborn*. 4th ed. Philadelphia, Pa: JB Lippincott; 1994. 1211-28.
41. Kim SY, Helman LJ. Strategies to Explore New Approaches in the Investigation and Treatment of Osteosarcoma. *Cancer Treat Res*. 2010. 152:517-528.
42. Clark JC, Dass CR, Choong PF. A review of clinical and molecular prognostic factors in osteosarcoma. *J Cancer Res Clin Oncol*. 2008 Mar. 134(3):281-97.
43. Pochanugool L, Subhadharaphandou T, Dhanachai M, et al. Prognostic factors among 130 patients with osteosarcoma. *Clin Orthop Relat Res*. 1997 Dec. 345:206-14.
44. Tsuchiya H, Tomita K. Prognosis of osteosarcoma treated by limb-salvage surgery: the ten-year intergroup study in Japan. *Jpn J Clin Oncol*. 1992 Oct. 22(5):347-53.
45. Taylor WF, Ivins JC, Unni KK, et al. Prognostic variables in osteosarcoma: a multi-institutional study. *J Natl Cancer Inst*. 1989 Jan 4. 81(1):21-30.
46. Hudson M, Jaffe MR, Jaffe N, et al. Pediatric osteosarcoma: therapeutic strategies, results, and prognostic factors derived from a 10-year experience. *J Clin Oncol*. 1990 Dec. 8(12):1988-97.
47. Meyer WH, Schell MJ, Kumar AP, et al. Thoracotomy for pulmonary metastatic osteosarcoma. An analysis of prognostic indicators of survival. *Cancer*. 1987 Jan 15. 59(2):374-9.
48. Yang J, Yang D, Cogdell D, Du X, Li H, Pang Y, et al. APEX1 gene amplification and its protein overexpression in osteosarcoma: correlation with recurrence, metastasis, and survival. *Technol Cancer Res Treat*. 2010 Apr. 9(2):161-9.
49. <http://emedicine.medscape.com/article/1256857-overview>

50. Song WS, Kong CB, Jeon DG, Cho WH, Kim MS, Lee JA, et al. Prognosis of extremity osteosarcoma in patients aged 40-60 years: A cohort/case controlled study at a single institute. *Eur J Surg Oncol.* 2010 Apr 2.
51. Rahman I, Biswas SK, Kirkham PA. Regulation of inflammation and redox signaling by dietary polyphenols. *Biochem Pharmacol.* 2006;72:1439-52.
52. Vogel P (1815) *J Pharm* 50
53. Daybe FV (1870) *Über Curcumin, den Farbstoff der Curcumawurzel.* 609
54. Aggarwal BB, Sethi G, Baladandayuthapani V, Krishnan S, Shishodia S. Targeting cell signaling pathways for drug discovery: an old lock needs a new key. *J Cell Biochem.* 2007;102:580-92.
55. Huang MT, Wang ZY, Georgiadis CA, Laskin JD, Conney AH. Inhibitory effects of curcumin on tumor initiation by benzo[a]pyrene and 7, 12-dimethylbenz[a]anthracene. *Carcinogenesis.* 1992; 13:2183-6.
56. Conney AH, Lysz T, Ferraro T, et al. Inhibitory effect of curcumin and some related dietary compounds on tumor promotion and arachidonic acid metabolism in mouse skin. *Adv Enzyme Regul.* 1991;31:385-96.
57. Huang MT, Smart RC, Wong CQ, Conney AH. Inhibitory effect of curcumin, chlorogenic acid, caffeic acid, and ferulic acid on tumor promotion in mouse skin by 12-O-tetradecanoylphorbol13-acetate. *Cancer Res.* 1988;48:5941-6.
58. Bilmen JG, Khan SZ, Javed MH, Michelangeli F. Inhibition of the SERCA Ca<sup>2+</sup> pumps by curcumin. Curcumin putatively stabilizes the interaction between the nucleotide-binding and phosphorylation domains in the absence of ATP. *Eur J Biochem.* 2001;268:6318-27.
59. Barry J, Fritz M, Brender JR, Smith PE, Lee DK, Ramamoorthy A. Determining the effects of lipophilic drugs on membrane structure by solid-state NMR spectroscopy: the case of the antioxidant curcumin. *J Am Chem Soc.* 2009;131:4490-8.
60. Epan RF, Martinou JC, Fornallaz-Mulhauser M, Hughes DW, Epan RM. The apoptotic protein tBid promotes leakage by altering membrane curvature. *J Biol Chem.* 2002;277:32632-9.
61. Jayaraj Ravindran, Sahdeo Prasad, and Bharat B. Aggarwal, Curcumin and Cancer Cells: How Many Ways Can Curry Kill Tumor Cells Selectively?, *The AAPS Journal*, 2009, 11: 3:495-510
62. Kerr JF, Wyllie AH, Currie AR. Apoptosis: a basic biological phenomenon with wide-ranging implications in tissue kinetics. *Br J Cancer* 1972;26:239-57.
63. Paweletz N. Walther Flemming: pioneer of mitosis research. *Nat Rev Mol Cell Biol* 2001;2:72-5.
64. Kerr JF. History of the events leading to the formulation of the apoptosis concept. *Toxicology* 2002;181-182:471-4.
65. Horvitz HR. Genetic control of programmed cell death in the nematode *Caenorhabditis elegans*. *Cancer Res* 1999;59:1701s-1706s.
66. Norbury CJ, Hickson ID. Cellular responses to DNA damage. *Annu Rev Pharmacol Toxicol* 2001;41:367-401.
67. Susan Elmore, Apoptosis: A Review of Programmed Cell Death, *Toxicol Pathol.* 2007 ; 35(4): 495-516
68. Hacker G. The morphology of apoptosis. *Cell Tissue Res* 2000;301:5-17. [PubMed: 10928277]
69. Igney FH, Krammer PH. Death and anti-death: tumour resistance to apoptosis. *Nat Rev Cancer* 2002;2:277-88.

70. Hengartner MO. The biochemistry of apoptosis. *Nature* 2000;407:770–6.
71. Cohen GM. Caspases: the executioners of apoptosis. *Biochem J* 1997;326(Pt 1):1–16.
72. Rai NK, Tripathi K, Sharma D, Shukla VK. Apoptosis: a basic physiologic process in wound healing. *Int J Low Extrem Wounds* 2005;4:138–44.
73. Bratton DL, Fadok VA, Richter DA, Kailey JM, Guthrie LA, Henson PM. Appearance of phosphatidylserine on apoptotic cells requires calcium-mediated nonspecific flip-flop and is enhanced by loss of the aminophospholipid translocase. *J Biol Chem* 1997;272:26159–65.
74. Arur S, Uche UE, Rezaul K, Fong M, Scranton V, Cowan AE, Mohler W, Han DK. Annexin I is an endogenous ligand that mediates apoptotic cell engulfment. *Dev Cell* 2003;4:587–98.
75. Locksley RM, Killeen N, Lenardo MJ. The TNF and TNF receptor superfamilies: integrating mammalian biology. *Cell* 2001;104:487–501.
76. Ashkenazi A, Dixit VM. Death receptors: signaling and modulation. *Science* 1998;281:1305–8.
77. Chicheportiche Y, Bourdon PR, Xu H, Hsu YM, Scott H, Hession C, Garcia I, Browning JL. TWEAK, a new secreted ligand in the tumor necrosis factor family that weakly induces apoptosis. *J Biol Chem*, 1997;272:32401–10.
78. Peter ME, Krammer PH. Mechanisms of CD95 (APO-1/Fas)- mediated apoptosis. *Curr Opin Immunol*, 1998;10:545–51.
79. Suliman A, Lam A, Datta R, Srivastava RK. Intracellular mechanisms of TRAIL: apoptosis through mitochondrial-dependent and -independent pathways. *Oncogene* 2001;20:2122–33.
80. Hsu H, Xiong J, Goeddel DV. The TNF receptor 1-associated protein TRADD signals cell death and NfκB activation. *Cell* 1995;81:495–504.
81. Wajant H. The Fas signaling pathway: more than a paradigm. *Science* 2002;296:1635–6. [PubMed: 12040174]
82. Kischkel FC, Hellbardt S, Behrmann I, Germer M, Pawlita M, Krammer PH, Peter ME. Cytotoxicity-dependent APO-1 (Fas/CD95)- associated proteins form a death-inducing signaling complex (DISC) with the receptor. *Embo J* 1995;14:5579–88. [PubMed: 8521815]
83. Slee EA, Adrain C, Martin SJ. Executioner caspase-3, -6, and -7 perform distinct, non-redundant roles during the demolition phase of apoptosis. *J Biol Chem* 2001;276:7320–6.
84. Sakahira H, Enari M, Nagata S. Cleavage of CAD inhibitor in CAD activation and DNA degradation during apoptosis. *Nature* 1998;391:96–9.
85. Kothakota S, Azuma T, Reinhard C, Klippel A, Tang J, Chu K, McGarry TJ, Kirschner MW, Kohts K, Kwiatkowski DJ, Williams LT. Caspase-3-generated fragment of gelsolin: effector of morphological change in apoptosis. *Science* 1998;281:100–3.
86. Ferraro-Peyret C, Quemeneur L, Flacher M, Revillard JP, Genestier L. Caspase-independent phosphatidylserine exposure during apoptosis of primary T lymphocytes. *J Immunol* 2002;169:4805–10.
87. Mandal D, Mazumder A, Das P, Kundu M, Basu J. Fas-, caspase-8-, and caspase-3-dependent signalling regulates the activity of the aminophospholipid translocase and phosphatidylserine externalization in human erythrocytes. *J Biol Chem* 2005;280:39460–7.
88. Fadok VA, de Cathelineau A, Daleke DL, Henson PM, Bratton DL. Loss of phospholipid asymmetry and surface exposure of phosphatidylserine is required for phagocytosis of apoptotic cells by macrophages and fibroblasts. *J Biol Chem* 2001;276:1071–7.
89. <http://www.uniprot.org/uniprot/Q04206>, 2017.07.03
90. <http://www.uniprot.org/uniprot/Q04206>
91. <http://www.abcam.com/mts-cell-proliferation-assay-kit-colorimetric-ab197010.html>, 2017.07.03

92. <https://www.aceabio.com/product/rtca-dp/>, 2017.07.03
93. [http://docs.abcam.com/pdf/protocols/Introduction\\_to\\_flow\\_cytometry\\_May\\_10.pdf](http://docs.abcam.com/pdf/protocols/Introduction_to_flow_cytometry_May_10.pdf), 2017.07.03
94. <https://www.ncbi.nlm.nih.gov/pmc/articles/PMC4579552/>, 2017.07.03
95. <https://www.biolegend.com/en-us/products/apc-annexin-v-apoptosis-detection-kit-with-7-aad-9754>, 2017.07.03
96. <https://www.rndsystems.com/products/proteome-profiler-antibody-arrays?gclid=CPvp3NKb8NQCFQngGwod6I8HsQ>, 2017.07.03
97. <https://www.applichem.com/en/products/laboratory-biochemicals/electrophoresis/>, 2017.07.03
98. Fong YC, Yang WH, Hsu SF, Hsu HC, Tseng KF, Hsu CJ, et al. 2-Methoxyestradiol induces apoptosis and cell cycle arrest in human chondrosarcoma cells. *J Orthop Res* 2007;25:1106–14.
99. Aggarwal BB, Shishodia S. Molecular targets of dietary agents for prevention and therapy of cancer. *Biochem Pharmacol* 2006;71:1397–421.
100. Anand P, Sundaram C, Jhurani S, Kunnumakkara AB, Aggarwal BB. Curcumin and cancer: an "old-age" disease with an "age-old" solution. *Cancer Lett* 2008;267:133–64.
101. Goel A, Kunnumakkara AB, Aggarwal BB. Curcumin as "Curecumin": from kitchen to clinic. *Biochem Pharmacol* 2008;77:1325–32.
102. Dazhi Yu, Fengmei An, Xu He, Xuecheng Cao; Curcumin inhibits the proliferation and invasion of human osteosarcoma cell line MG-63 by regulating miR-138. *Int J Clin Exp Pathol*. 2015; 8(11): 14946–14952
103. Run chang, linlin sun, Thomas J Webster. Short communication: selective cytotoxicity of curcumin on osteosarcoma cells compared to healthy osteoblasts. *J Nanomedicine*. 2014; 9: 461–465.
104. Santosh S Dhule, Patrice Penfornis, Jibao He, Michael R Harris, Treniece Terry, Vijay John, and Radhika Pochampally. The Combined Effect of Encapsulating Curcumin and C6 Ceramide in Liposomal Nanoparticles against Osteosarcoma. *Mol Pharm*. 2014 Feb 3; 11(2): 417–427.
105. Fu Z, Chen X, Guan S, Yan Y, Lin H, Hua ZC, Curcumin inhibits angiogenesis and improves defective hematopoiesis induced by tumor-derived VEGF in tumor model through modulating VEGF-VEGFR2 signaling pathway. *Oncotarget*. 2015 Aug 14;6(23):19469-82.
106. Lee HP, Li TM, Tsao JY, Fong YC, Tang CH. Curcumin induces cell apoptosis in human chondrosarcoma through extrinsic death receptor pathway. *Int Immunopharmacol*. 2012 Jun;13(2):163-9.
107. Dennis Ma, Phillip Tremblay, Kevinjeet Mahngar, Jonathan Collins, Tomas Hudlicky, Siyaram Pandey. Selective Cytotoxicity against Human Osteosarcoma Cells by a Novel Synthetic C-1 Analogue of 7-Deoxypancratistatin Is Potentiated by Curcumin. *PLoS One*. 2011;6(12):e28780.
108. Orr WS, Denbo JW, Saab KR, Ng CY, Wu J, Li K, Garner JM, Morton CL, Du Z, Pfeffer LM, Davidoff AM. Curcumin potentiates rhabdomyosarcoma radiosensitivity by suppressing NF- $\kappa$ B activity. *PLoS One*. 2013;8(2):e51309.
109. Saleh EM1, El-Awady RA, Anis N, El-Sharkawy N. Induction and repair of DNA double-strand breaks using constant-field gel electrophoresis and apoptosis as predictive markers for sensitivity of cancer cells to cisplatin. *Induction and repair of DNA double-strand breaks using constant-field gel electrophoresis and apoptosis as predictive markers for sensitivity of cancer cells to cisplatin*.
110. Bush, J.A.; Cheung, K.J., Jr.; Li, G. Curcumin induces apoptosis in human melanoma cells through a Fas receptor/caspase-8 pathway independent of p53. *Exp. Cell. Res*. 2001, 271, 305–314.
111. Moragoda, L.; Jaszewski, R.; Majumdar, A.P. Curcumin induced modulation of cell cycle and apoptosis in gastric and colon cancer cells. *Anticancer Res*. 2001, 21, 873–878.
112. [file:///D:/Users/Sepp/Downloads/sc-7977%20\(1\).pdf](file:///D:/Users/Sepp/Downloads/sc-7977%20(1).pdf)

113. Baeuerle PA, Baltimore D. NF-kappa B: ten years after. *Cell*. 1996;87:13–20.
114. Vlahopoulos SA, Cen O, Hengen N, Agan J, Moschovi M, Critselis E, Adamaki M, Bacopoulou F, Copland JA, Boldogh I, Karin M, Chrousos GP (August 2015). "Dynamic aberrant NF-κB spurs tumorigenesis: a new model encompassing the microenvironment". *Cytokine & Growth Factor Reviews*. 26 (4): 389–403.
115. Escárcega RO, Fuentes-Alexandro S, García-Carrasco M, Gatica A, Zamora A (March 2007). "The transcription factor nuclear factor-kappa B and cancer". *Clinical Oncology*. 19 (2): 154–61
116. Yu D, An F, He X, Cao X. Curcumin inhibits the proliferation and invasion of human osteosarcoma cell line MG-63 by regulating miR-138. *Int J Clin Exp Pathol*. 2015 Nov 1;8(11):14946-52.
117. Wilken R, Veena MS, Wang MB, Srivatsan ES. Curcumin: A review of anti-cancer properties and therapeutic activity in head and neck squamous cell carcinoma. *Mol Cancer*. 2011 Feb 7;10:12.
118. Jobin, C.; Bradham, C.A.; Russo, M.P.; Juma, B.; Narula, A.S.; Brenner, D.A.; Sartor, R.B. Curcumin blocks cytokine-mediated NF-kappa B activation and proinflammatory gene expression by inhibiting inhibitory factor I-kappa B kinase activity. *J. Immunol*. 1999, 163, 3474–3483.
119. Bharti, A.C.; Donato, N.; Singh, S.; Aggarwal, B.B. Curcumin (diferuloylmethane) downregulates the constitutive activation of nuclear factor-kappa B and IκappaB kinase in human multiple myeloma cells, leading to suppression of proliferation and induction of apoptosis. *Blood* 2003, 101, 1053–1062.
120. Siwak, D.R.; Shishodia, S.; Aggarwal, B.B.; Kurzrock, R. Curcumin-induced antiproliferative and proapoptotic effects in melanoma cells are associated with suppression of IκappaB kinase and nuclear factor kappaB activity and are independent of the B-Raf/mitogenactivated/extracellular signal-regulated protein kinase pathway and the Akt pathway. *Cancer* 2005, 104, 879–890.
121. Shishodia, S.; Potdar, P.; Gairola, C.G.; Aggarwal, B.B. Curcumin (diferuloylmethane) downregulates cigarette smoke-induced NF-kappaB activation through inhibition of IκappaB kinase in human lung epithelial cells: Correlation with suppression of COX-2, MMP-9 and cyclin D1. *Carcinogenesis* 2003, 24, 1269–1279.
122. Deeb, D.; Jiang, H.; Gao, X.; Al-Holou, S.; Danyluk, A.L.; Dulchavsky, S.A.; Gautam, S.C. Curcumin [1,7-bis(4-hydroxy-3-methoxyphenyl)-1-6-heptadine-3,5-dione; C21H20O6] sensitizes human prostate cancer cells to tumor necrosis factor-related apoptosis-inducing ligand/Apo2L-induced apoptosis by suppressing nuclear factor-kappaB via inhibition of the pro-survival Akt signaling pathway. *J. Pharmacol. Exp. Ther*. 2007, 321, 616–625.
123. Dhandapani, K.M.; Mahesh, V.B.; Brann, D.W. Curcumin suppresses growth and chemoresistance of human glioblastoma cells via AP-1 and NFκappaB transcription factors. *J. Neurochem*. 2007, 102, 522–538.
124. Sharma, C.; Kaur, J.; Shishodia, S.; Aggarwal, B.B.; Ralhan, R. Curcumin down regulates smokeless tobacco-induced NF-kappaB activation and COX-2 expression in human oral premalignant and cancer cells. *Toxicology* 2006, 228, 1–15.
125. Milacic, V.; Banerjee, S.; Landis-Piwowar, K.R.; Sarkar, F.H.; Majumdar, A.P.; Dou, Q.P. Curcumin inhibits the proteasome activity in human colon cancer cells in vitro and in vivo. *Cancer Res*. 2008, 68, 7283–7292.
126. Yang, H.; Landis-Piwowar, K.R.; Chen, D.; Milacic, V.; Dou, Q.P. Natural compounds with proteasome inhibitory activity for cancer prevention and treatment. *Curr. Protein Pept. Sci*. 2008, 9, 227–239.
127. Landis-Piwowar, K.R.; Milacic, V.; Chen, D.; Yang, H.; Zhao, Y.; Chan, T.H.; Yan, B.; Dou, Q.P. The proteasome as a potential target for novel anticancer drugs and chemosensitizers. *Drug Resist. Update*. 2006, 9, 263–273.
128. Walsby E, Pearce L, Burnett AK, Fegan C, Pepper C. The Hsp90 inhibitor NVP-AUY922-AG inhibits NF-κB signaling, overcomes microenvironmental cytoprotection and is highly synergistic with fludarabine in primary CLL cells. *Oncotarget*. 2012;3:525–534.
129. Salem K, Brown CO, Schibler J, Goel A. Combination chemotherapy increases cytotoxicity of multiple myeloma cells by modification of nuclear factor (NF)-κB activity. *Exp Hematol*. 2013;41:209–218. doi: 10.1016/j.exphem.2012.10.002.

130. Jiang X-J, Huang K-K, Yang M, Qiao L, Wang Q, Ye J-Y, Zhou H-S, Yi Z-S, Wu F-Q, Wang Z-X, Zhao Q-X, Meng F-Y. Synergistic effect of panobinostat and bortezomib on chemoresistant acute myelogenous leukemia cells via AKT and NF- $\kappa$ B pathways. *Cancer Letters*. 2012;326:135–142. doi: 10.1016/j.canlet.2012.07.030.
131. Katsman A, Umezawa K, Bonavida B. Chemosensitization and immunosensitization of resistant cancer cells to apoptosis and inhibition of metastasis by the specific NF-kappaB inhibitor DHMEQ. *Curr Pharm Des*. 2009;15:792–808. doi: 10.2174/138161209787582156.
132. Abaza MSI, Bahman AM, Al-Attayah RJ, Kollamparambil AM. Synergistic induction of apoptosis and chemosensitization of human colorectal cancer cells by histone deacetylase inhibitor, scriptaid, and proteasome inhibitors: potential mechanisms of action. *Tumour Biol*. 2012;33:1951–1972. doi: 10.1007/s13277-012-0456-6.
133. Fuchs O. Transcription factor NF- $\kappa$ B inhibitors as single therapeutic agents or in combination with classical chemotherapeutic agents for the treatment of hematologic malignancies. *Curr Mol Pharmacol*. 2010;3:98–122.
134. McConkey DJ, Zhu K. Mechanisms of proteasome inhibitor action and resistance in cancer. *Drug Resist Updat*. 2008;11:164–179. doi: 10.1016/j.drug.2008.08.002.

## 6 List of Abbreviations

STS	soft tissue sarcoma
SS	synovial sarcoma
OS	osteosarcoma
DMEM-F12	Dulbecco's modified Eagle's medium F12
FBS	fetal bovine serum
CO <sub>2</sub>	carbon dioxide
H <sub>2</sub> O	water
EtOH	ethanol
PBS	phosphate-buffered saline
FSC	forward scatter
SSC	side scatter
Rb	retinoblastoma
DISC	death-inducing signaling complex
FADD	Fas-associated protein with death domain
TNFR 1	tumor necrosis factor receptor
PARP	poly(ADP-ribose)-Polymerase
H2AX	histon H2AX
STR	short tandem repeat
DAPI	4',6-Diamidin-2-phenylindol
qPCR	quantitative Real-time Polymerase Chain Reaction
RNA	ribonucleic acid
DNA	deoxyribonucleic acid
NFW	nuclease free water

SDS	sodium dodecyl sulfate
APS	ammoniumperoxodisulfate
TEMED	tetramethylethyldiamin
ECL	electrochemiluminescence

## 7 List of Figures

Figure 1: Tumor clonality.....	2
Figure 2: Stages of tumor development.....	3
Figure 3: Chemical structure of curcumin.....	7
Figure 4: Schematic representation of apoptotic events.....	9
Figure 5: Extrinsic pathway of apoptosis.....	11
Figure 6: NF-kappa-B signaling pathway.....	14
Figure 7: The pipetting-layout of the vimentin-DAPI staining.....	18
Figure 8: Structures of MTS tetrazolium and its formazan product.....	20
Figure 9: Overview of cellular impedance apparatus.....	21
Figure 10: Overview of the flow cytometer.....	22
Figure 11: Steps of RNA isolation.....	25
Figure 12: Experimental steps of western blotting from sample preparation to Protein electrophoresis.....	37
Figure 13: Two electro-transfer techniques: the wet transfer and the semi-dry transfer.....	38
Figure 14: The antibody incubation process of western blotting after protein transfer onto the membrane.....	40
Figure 15: Vimentin-DAPI immunofluorescence staining of the SW-982 cell line.....	43
Figure 16: Vimentin-DAPI immunofluorescence staining of the U2OS cell line.....	43
Figure 17: Influence of DMAS on cell viability of chondrosarcoma cell lines SW-982 (A), SW-1353 (B), U2OS (C) and TE-671 (D).....	44
Figure 18: IC50-values of the sarcoma cell lines SW-982 and U2OS for 48 h without (A, C) and with (B, D) exchange of the culture medium before measurement.....	46
Figure 19: Influence of curcumin on cell proliferation of sarcoma cell lines SW-982 (A) and U2OS (B).....	47
Figure 20: Results from the cleaved caspase 3 measurement of the SW-982 cells.....	48
Figure 21: Results from the cleaved caspase 3 measurement of the U2OS cells.....	49

Figure 22: Curcumin did not induce apoptosis in SW-982 (A) and U2OS (B) cells.....	50
Figure 23: NFκB assay of untreated and treated SW-982 cells (A) and U2OS cells (B).....	51
Figure 24: Relative gene expression levels of FADD, FAS, DR4 and TNFR1 in untreated and treated (curcumin) SW-982 and U2OS cells.....	52
Figure 25: Gene expression of H2AX (A), PARP and cleaved PARP (B) in untreated and treated (curcumin) SW-982 and U2OS cells.....	53
Figure 26: Gene expression of unphosphorylated and phosphorylated IκB-α in untreated and treated (curcumin) SW-982 and U2OS cells.....	54
Figure 27: Gene expression of unphosphorylated and phosphorylated p65 and p50 in untreated and treated (curcumin) SW-982 and U2OS cells.....	55
Figure 28: Inactive (unphosphorylated) IκB-α inhibits NFκB heterodimer p65/p50.....	58

# 8 List of Tables

Table 1: Recommended acrylamide concentration for protein target within defined size ranges .....32

Table 2: Recipes of gels.....33

Table 3: Volume list for the preparation of different albumin standard dilutions.....36

Table 4: STR loci comparison of SW-982 cells .....41

Table 5: STR loci comparison of U2OS cells.....42

Table 6: Mean ± SD and p-values of MTS proliferation assay of all time points of the U2OS cell line.....43

Table 7: Mean ± SD and p-values of MTS proliferation assay of all time points of the SW-982 cell line.....43

Table 6: Results from the cleaved caspase 3 measurement of the SW-982 and U2OS cells.....49